Seeing is believing – quantifying is convincing: Computational image analysis in biology*

Ivo F. Sbalzarini
MOSAIC Group, Chair of Scientific Computing for Systems Biology,
Faculty of Computer Science, TU Dresden
& Center for Systems Biology Dresden
& Max Planck Institute of Molecular Cell Biology and Genetics,
Pfotenhauerstr. 108, D–01307 Dresden, Germany.

Abstract

Imaging is center stage in biology. Advances in microscopy and labeling techniques have enabled unprecedented observations and continue to inspire new developments. Efficient and accurate quantification and computational analysis of the acquired images, however, are becoming the bottleneck. We review different paradigms of computational image analysis for intracellular, single-cell, and tissue-level imaging, providing pointers to the specialized literature and listing available software tools. We place particular emphasis on clear categorization of image-analysis frameworks and on identifying current trends and challenges in the field. We further outline some of the methodological advances that are required in order to use images as quantitative scientific measurements.

KEYWORDS: image analysis, microscopy, bio-image informatics, image quantification, computational image analysis, bio-image software

1 Introduction

"Seeing is believing" is an old saying in microscopy. With the classical biochemical methods being increasingly complemented by imaging techniques, however, the subjective interpretation of what one sees in a microscopy image gets in the way of scientific reproducibility and logical deduction. Arguments such as "I saw it that way" or "it looked like" become less tolerable as conclusions are based on image data. Positing that the images are correctly acquired and free of artifacts (North, 2006), one hence wishes to reduce, or at least quantify, viewer bias and subjective expectations and beliefs by extracting reproducible numbers from the images.

Together with the need to process ever-larger sets of images at high throughput, reproducible quantification motivates the use of computational image analysis (Eils and Athale, 2003; Myers, 2012). Having a computer software do the image analysis renders the results reproducible. If the same software is run twice on the same image, the same result is produced. Manual analysis, however, is often not reproducible, as different people would quantify the image differently and even the same person might attribute slightly different numbers to the same object upon different repetitions of the analysis. Computational analysis also increases the throughput, as thousands of images can be processed, potentially even in parallel on a computer cluster. A third reason for using computational image analysis it that algorithms can detect minute pixel variations that the human eye cannot see (Danuser, 2011). Finally, results from computational image analysis, such as cell shapes and fluorescence distributions, can be directly used to build systems models and computer simulations of biological processes (Sbalzarini, 2013). Such simulations can then test whether the hypothesized, simulated mechanism is *sufficient* to produce the experimentally observed behavior. Perturbation experiments can then show whether it is also *necessary*. Image analysis is hence the first step toward a systems understanding of spatiotemporal biological processes.

*This preprint has been published as a book chapter in: "Focus on Bio-Image Informatics", Springer Series on Advances in Anatomy, Embryology and Cell Biology, Chapter 1, pp. 1–39, Springer, 2016.

Image analysis is a large and complex field, intersecting with *image processing* and *computer vision*. Image processing is a branch of signal processing, interpreting images as multi-dimensional continuous or discrete signals. Computer vision is the branch of artificial intelligence that tries to teach computers to "see", i.e., to interpret images. Computer vision has a forty-year history and is a well-researched field. Importing techniques from computer vision can help solve problems in biological image analysis (Danuser, 2011). Nevertheless, computer vision is not a panacea for bio-image analysis, because computer vision has evolved with different images and goals in mind. The focus in computer vision is on interpreting complex scenes from images with good resolution and signal, i.e., conditions under which also the human eye operates. Such images are typically acquired with digital photo cameras and show objects that are much larger than the wavelength of the light used to image them. This has the important consequences that diffraction effects can be neglected and that imaging noise can be modeled as Gaussian, as the photon count per pixel is high. These assumptions pose challenges to computational analysis that are different from those for images acquired in microscopy. Microscopy images are typically characterized by low signal-to-noise ratios and significant diffraction artifacts. Moreover, the noise is frequently not Gaussian. Low-signal detectors such as (EM-)CCD and CMOS cameras, as well as photo-multiplier tubes and photodiodes, produce dominant Poisson noise, which is overlaid with the Gaussian noise from the electronics. Finally, microscopy frequently acquires 3D or 4D images, whereas digital photography is mostly limited to 2D. The specifics of biological images and their analysis have given rise to the new discipline of *bio-image informatics* (Peng, 2008; Myers, 2012).

Despite significant advances in the past years, bio-image informatics is still in its early days, and many challenges remain to be addressed. This includes the development of algorithms and software that better utilize the available computer resources in order to allow high-throughput studies and high resolution with large multi-dimensional image data. Second, the topic of uncertainty quantification needs to be addressed, which has so far been poorly dealt with in bio-imaging. If the goal is to be quantitative, i.e., to use imaging and image analysis as *measurements* in the scientific sense (Dietrich, 1991), one has to know and quantify the measurement errors and their propagation and amplification along the analysis pipeline. Simply having an algorithm that tells us "here is a nucleus" is not of much use in big-data studies, and it prohibits statistical tests on the results. We need to know the probability that there is a nucleus, and the probability that the algorithm failed or produced a wrong detection. Third, we need to develop versatile frameworks and algorithms that can be adapted to different applications without having to re-write the software on a case-by-case basis. This requires theoretical and algorithmic frameworks that are adapted to the specifics of biological images and provide us with systematic and principled ways of including prior knowledge about the imaging process and the imaged objects into the analysis. Fourth, the new algorithms need to be made available to the community as user-friendly, open-source software. These four current challenges equally apply to all image-analysis paradigms and all imaging modalities.

Light microscopy is probably the prevalent imaging modality in biology today, as it allows live-cell imaging and real-time observation (Royer et al, 2015) of dynamic processes in cells and tissues. Focusing on fluorescence microscopy, we discuss the above four challenges and show for each of them where the field currently stands and what remains to be addressed. First, however, we outline the different paradigms of image analysis, providing a scaffold to structure the discussion. We close this article by highlighting different design approaches and current trends in bio-image analysis software tools, and by summarizing and generalizing our observations.

2 Computational bio-image analysis

Bio-image informatics enables us to address biological questions that could not be addressed otherwise, or only at a much higher cost (Peng, 2008; Myers, 2012). These questions are naturally posed in terms of biological entities and concepts, such as "do cells in the vicinity of a dividing cell have a higher propensity to divide next during tissue growth?" Bio-image analysis has to bridge the gap between the biological question and the image data. Questions like what it means for a cluster of pixels in an image to be considered a "cell", how "vicinity" is measured over the pixel grid of an image, and what cell division "looks" like in the table of pixel intensity numbers need to be addressed and formulated as algorithmic recipes that can be programmed into a computer. This entails addressing the "what is where" inference problem over images, just as computer vision does. Quantitative bio-image analysis additionally needs to address the "how much of what is where" problem. This is harder, as more ambiguities exist. Due to the diffraction limit, for example, it is not always possible to distinguish the diffraction-limited bright spot created by a 50 nm object with high fluorophore concentration

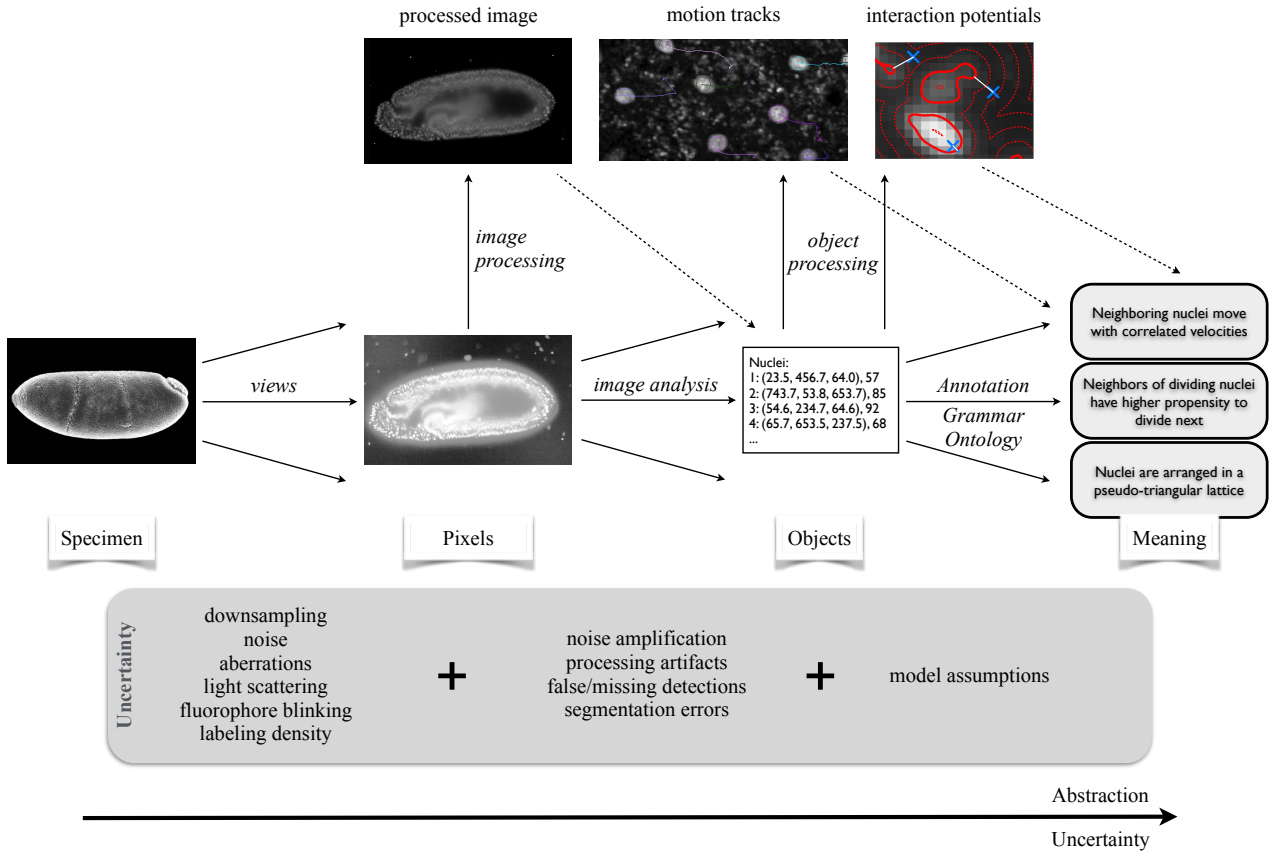

Figure 1: Data representation and uncertainties in image analysis. The same specimen can be imaged in different views, giving rise to different images. Image analysis extracts quantitative information from the image, which can then be interpreted to form conclusions. Every step increases the level of abstraction and adds uncertainties and errors that often remain uncharacterized. Dashed arrows indicate routes of additional processing. (Image sources: "Specimen" image from FlyBase.org; "Pixels" image courtesy of Pavel Tomancak, MPI-CBG; "processed image", "motion tracks", and "interaction potentials" by Yuanhao Gong, Pietro Incardona, and Jo Helmuth, respectively, all MOSAIC Group.)

from that created by a 200 nm object with lower fluorophore concentration. This becomes an issue when one is interested in quantifying the concentration of the labeled protein in small sub-cellular structures (e.g., endosomes) as a biologically meaningful readout (Helmuth et al, 2009). Unique answers can only be found when including problem-specific prior knowledge and calibration into the analysis.

2.1 From specimen to pixels to objects to meaning

Image analysis is a *data representation problem*, as illustrated in Fig. 1. The information for the final conclusion is already contained in the original specimen, albeit in a very different data representation.

Multiple steps are required working one's way through the data representation hierarchy from the specimen to meaning. The first step is image acquisition. The specimen can be imaged in many different ways, for example using different imaging modalities, different microscopes, different magnifications, different viewing angles, and different fluorescent markers. We call a specific imaging setup a *view*, leading to a digital image represented as a table of numerical pixel-intensity values. This clearly amounts to information loss, as many different images could be produced from one and the same specimen. Moreover, the intensity values in the pixel matrix are not easily related to actual fluorophore concentrations, since the microscope optics have an imperfect impulse-response function (Hecht, 2001), called the *point spread function* (PSF), the excitation light intensity may be unknown, and light is absorbed and scattered as it propagates through the sample. In order to bridge to biological meaning, the matrix of pixels hence needs to be interpreted in terms of the objects represented in the image, which can be done using different approaches, as discussed in the following.

All approaches are commonly referred to as *image analysis*, which aims to extract semantic meaning from images. Image analysis hence takes an image as input and produces object representations as output, for example a list of nuclei positions and sizes, or a 3D representation of cell shapes in a tissue. After image analysis, the information is hence no longer encoded in pixel matrices, but explicitly available as biologically tangible objects. This is in contrast to *image processing*, which transforms one image into another image that has, for example, less noise or blur. Examples include image deconvolution and contrast enhancement. Image processing is a sub-field of signal processing and operates within the image domain. *Image restoration* is a sub-field of image processing that aims to transform an image into one where the uncertainties and errors introduced by the image-acquisition process are reduced.

Image analysis often implies delineating objects represented in the image, a process called *image segmentation*. *Object detection* is a sub-task of segmentation that finds occurrences of the objects of interest in the image, and maybe counts them, but does not quantify their shapes. *Spatial pattern analysis* uses the detected and/or segmented objects to ask the question whether their spatial distribution is random or follows a certain pattern (Lagache et al, 2013). *Interaction analysis* is a special case of spatial pattern analysis, asking whether the distribution of one type of objects (e.g., viruses) is independent of the distribution of another type of objects (e.g., endosomes) and, if not, what hypothetical interaction between the two best explains their observed relative distribution (Helmuth et al, 2010; Lagache et al, 2015). An important analysis in time-lapse video is *motion tracking*, aiming at following moving objects over time and extracting their trajectories. This requires determining object correspondences across time points and is usually done after object detection or segmentation. Given the detected or segmented objects in each frame of a movie, tracking answers the question which detection in one frame corresponds to which detection in the next frame in the sense that the two are images of the same real-world object at different time points (Bar-Shalom and Blair, 2000). A wealth of tracking methods exist in biological imaging, both for particle tracking (compared and reviewed in (Chenouard et al, 2014)) and for cell tracking (compared and reviewed in (Maška et al, 2014)). Most of them have by now been integrated in standard software packages. The extracted trajectories of moving objects are rich sources of information about dynamics, types of motion (Sbalzarini and Koumoutsakos, 2005; Wieser et al, 2008; Ruprecht et al, 2011), and motion patterns (Helmuth et al, 2007). This has, for example, been used to analyze virus motion on and inside infected host cells (Ewers et al, 2005; Helmuth et al, 2007; Yamauchi et al, 2011) and to analyze the mobility of single molecules in plasma membranes (Wieser and Schütz, 2008). For spatially extended objects, one can also track the deformations of their outlines. This involves determining which point on an outline corresponds to which point on the later outline. Solutions based on mechanical ball-and-spring models (Machacek and Danuser, 2006) and level-set methods (Shi and Karl, 2005; Machacek and Danuser, 2006) have successfully been applied. Level-set methods (Sethian, 1999) have been used to track high-resolution outlines of polarizing and migrating keratocyes in phase-contrast movies (Ambühl et al, 2012), and to segment and track fluorescent HeLa and CHO cells (Dzyubachyk et al, 2010). This allows quantifying cells, their shapes, and temporal dynamics.

From this quantitative information about the shapes, positions, spatial distributions, and motion of the imaged objects, the researcher needs to derive biological meaning and new knowledge. Such meaning may come in the form of *annotations* of the objects found in the image (e.g., "this bright blob of pixels is a nucleus"), *grammar* (e.g., "nuclei are inside cells"), or *semantics* (e.g., "if a nucleus looks condensed and bright, the cell is entering mitosis"). This high-level interpretation of the image is application-specific and necessarily includes prior knowledge about what has been imaged. Otherwise, an image of fluorescently labeled virus particles on a cell membrane would be hard to distinguish from a photograph of the starry sky at night.

Including prior knowledge and interpreting the data inevitably introduces uncertainty. Indeed, errors and uncertainties are introduced at *every* stage of the image-analysis process and are propagated downstream. This includes uncertainties in the specimen itself, such as unknown labeling densities and blinking fluorophores (Annibale et al, 2011). Additional uncertainties are introduced by the view, i.e., the image acquisition process. This includes light scattering in the sample, aberrations from the optics, and noise from the photon-detection process and the electronics in the camera. Image processing and analysis are also not perfect and may amplify noise, introduce false detections, quantification errors, and missed detections. This is not limited to computational image processing; also humans make mistakes when interpreting and quantifying images. Finally, the interpretation of the resulting information is subject to uncertainties, as we are often implicitly assuming a model that may not be correct. Ideally, all of these uncertainties and errors should be known and quantified, and their influence on downstream results are bounded. Else it is impossible to decide whether an observed difference between two analyzed images is due to biological differences in the specimen, or just due to analysis artifacts.

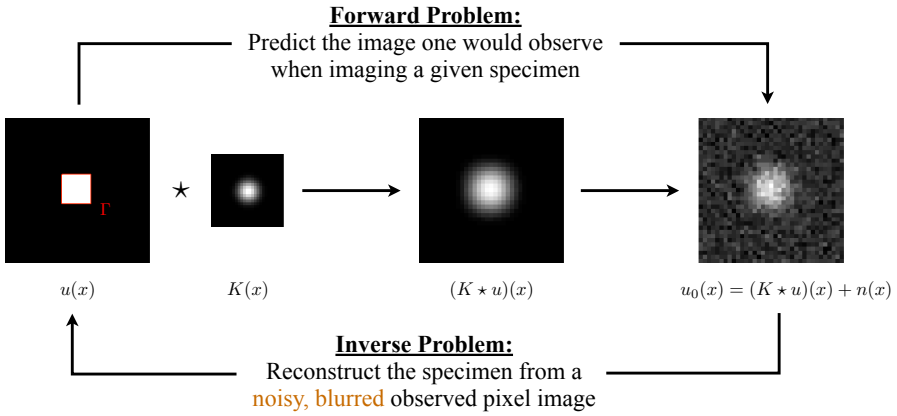

Figure 2: The forward and the inverse problem in fluorescence microscopy: the specimen $u(x)$ is imaged using optics with a certain point spread function $K(x)$, yielding a diffraction-limited, blurred image of the specimen. This image is then digitized onto the finite pixel grid of the camera, and the photon-counting process in the detector, as well as the camera electronics, introduce noise $n(x)$. Modeling this image-formation process, i.e., predicting the image for a known or hypothesized specimen is the *forward problem*. The *inverse problem* consists in reconstructing an unknown specimen or its delineating boundary Γ (red line) from a particular observed image $u_0(x)$. (Image source: Grégory Paul, MOSAIC Group).

2.2 The forward and the inverse problem

It is common to distinguish between the *forward problem* and the *inverse problem* in imaging, as illustrated in Fig. 2 for the case of fluorescence microscopy. The forward problem consists of finding a predictive model, the forward model, of the image-formation process. For a known or hypothesized specimen, this model predicts the image. The inverse problem entails reconstructing the specimen from a given observed image. Due to blur, noise, and other uncertainties introduced during image acquisition, there is usually no unique solution to the inverse problem, or its solution is unstable, which is why the inverse problem is called "ill-posed". A solution can only be found by including application-specific prior knowledge to *regularize* the problem. This prior knowledge can for example be the limit curvature of lipid membranes, or the PSF of the microscope. The solution space of the inverse problem is then restricted to those solutions that are compatible with the prior knowledge, eventually leading to a unique answer when sufficient prior knowledge is included.

The question arises, however, how much prior knowledge is required. In the absence of a closed theory, the pragmatic approach in bio-image analysis is to match the analysis aims and tools to the level of detail required by the biological question. Questions such as whether a co-localization study should account for fluorophore blinking and chromatic aberration, or not, are largely decided opportunistically with the final aim of the analysis in mind. This can be seen as a heuristic way of deciding which prior knowledge to include into the analysis.

2.3 Bayesian, or not?

Image analysis considers the inverse problem and is therefore an inference task. The goal is to infer shapes, locations, and distributions of the imaged objects from the acquired images. As in any inference task, there are two views of the problem: frequentist and Bayesian. Frequentist inference draws conclusions from the data by looking at frequencies of occurrence. For example, thresholding considers a pixel to be part of an object if its intensity is in the upper 10% of all pixels in the image. Bayesian inference draws conclusions that have high probability of explaining the data given the prior.

While both approaches include prior knowledge, e.g., about how the image has been acquired or the experimental design, the Bayesian approach formalizes the prior knowledge in the mathematical form of a Bayesian *prior*. *Prior knowledge* and a Bayesian *prior* are hence not the same, and in frequentist inference the former is present without the latter. In Bayesian inference, the inclusion of prior knowledge is not necessarily limited to the prior either, but may also enter other terms, such as the likelihood.

Bayesian inference is based on Bayes' theorem, as illustrated in Fig. 3. Applied to image segmentation, the theorem states that the segmentation that is most likely to produce the observed image when run through

Figure 3: Illustration of Bayes' theorem: we seek the segmentation that has the highest posterior probability of being correct given the observed image (blue). This can be achieved by maximizing the product of the likelihood of observing the image given the forward model output (red), and the prior knowledge about the imaged objects (green).

the given forward model is obtained by maximizing a quantity called the *posterior*, which is proportional to ($\propto$) the product of two known and computable terms: The first term is called the *likelihood* and it quantifies how likely it would be to observe the given image if the hypothetical segmentation were true. This is often done by measuring the difference between the observed image and the one predicted by the forward model for the hypothetical segmentation. The smaller this difference, the more likely the segmentation is. The second term is called the *prior* and it measures the *a-priori* probability that the hypothetical segmentation is correct, irrespective of the image observed. This could, e.g., attribute lower probability to membrane segmentations that are highly curved, formalizing our prior knowledge that lipid membranes tend to form smooth shapes.

All terms in Bayesian inference have the meaning of probabilities. However, given that in image analysis and experimentation it is often more natural to talk about *evidence* rather than *probability*, a theory like the Dempster-Shafer Evidence Theory might provide a more appropriate interpretation (Shafer, 1976). The key difference is that evidence does not have to sum up to 1, as probability does. Probability is the "chance" of there being two touching cells in the image, as opposed to a single cell. Evidence is the "degree of belief" that there is one or two cells. If the image is so blurry that one cannot decide whether it is one or two cells, one could give a low value to the probability of there being two cells. Since probabilities have to sum to 1, however, this implies a high probability that there is one cell. The statement hence inevitably becomes: "I am very certain that there is only one cell." This is not the same as: "I cannot decide whether there is one or two." If one cannot decide, this means there is neither compelling evidence for one, nor for two cells. Since evidence does not have to sum to 1, one could hence simultaneously give low evidence to *both* possibilities.

In summary, there are three inference frameworks for image analysis: frequentist inference, Bayesian inference, and evidence theory. The first two currently dominate the field.

3 Image analysis paradigms

Irrespective of the inference framework used, there are different philosophies and approaches to image analysis. Each of them has its own way of interpreting images and of including prior knowledge, and comes with its own set of advantages and caveats. The approach implemented in a given software largely defines what the software is in principle able to do, and what not. We discuss the three most prominent paradigms below, focusing on how to convert an image, stored as a matrix of pixel values, to quantitative information about the features and objects represented in it.

3.1 The filter-based paradigm

The filter-based approach to image analysis consists in applying a series of arithmetic operations to the pixel-intensity values in order to isolate or reveal objects of interest, or compute object segmentation masks. Prior knowledge is included in the filter design. In order to detect bright spots in an image, one could for example run a band-pass filter over the image to reduce noise and background, and then use a relative threshold filter to select all local maxima that are brighter than a given threshold (Crocker and Grier, 1996). More advanced approaches to spot detection use multi-scale wavelet filters (Olivo-Marin, 2002).

Filters are classified as linear and non-linear, shift-invariant and shift-variant, discrete (digital) and continuous (analog). Linear filters only compute linear combinations of the pixels in the input image, for example weighted

sums or differences. Non-linear filters apply arbitrary non-linear operations. Shift-invariant filters always perform the same operations regardless of *where* in the image they are applied. For example, they always compute the average of all neighbors of a pixel, regardless of which pixel is at the center. Shift-variant filters perform different operations depending on where they are shifted to, e.g. using a different PSF in different parts of the image. Discrete filters operate on discrete pixel lattices with discrete intensity levels, whereas continuous filters can also be evaluated at sub-pixel locations and may produce non-integer intensity values. Since digital images are discrete by nature, continuous filters are often based on assuming certain continuous basis functions, like Splines or Bézier curves. Any linear shift-invariant filter amounts to convolving the input image with a filter kernel and can hence be efficiently computed as a convolution.

Most filter-based approaches are found in image processing, including prominent examples such as the fast Fourier transform (Cooley and Tukey, 1965), wavelet transforms (Chan and Shen, 2005), thresholding (Otsu, 1975), edge-detection (Canny, 1986), anisotropic diffusion filters (Perona and Malik, 1990), and image naturalization (Gong and Sbalzarini, 2014) (see Fig. 4). A special case are the discrete filters used in mathematical morphology (Najman and Talbot, 2010). In image analysis, a famous filter-based method is watershed segmentation (Najman and Schmitt, 1996), which is a combination of linear shift-invariant filters to determine the seeds for a subsequent watershed transform (Meyer et al, 1997) from mathematical morphology. Filter-based approaches to motion tracking notably include those based on pixel cross-correlations (Willert and Gharib, 1991) and split/merge data-association filters, which are however often augmented with Bayesian model-based approaches for multi-hypothesis tracking (Genovesio and Olivo-Marin, 2004). Approaches combining Gaussian filtering with mathematical morphology and thresholding are routinely used for single-particle detection (Sbalzarini and Koumoutsakos, 2005) and filament segmentation (Ruhnow et al, 2011).

Due to their explicit nature, filter-based approaches are computationally fast. They are, however, typically specialized. Filter-based approaches are designed specifically to the task. They provide less flexibility to adapt to different tasks than machine-learning and model-based methods do. Moreover, filter-based approaches typically have a large number of parameters that need to be adjusted and tuned. Depending, for example, on how one sets the threshold in a thresholding filter, one can get any result one wants. Often, there is no good *a-priori* criterion to tune the parameters, leaving us with arguments like "it gave me what I wanted" or "it looked best" that fundamentally go against the idea of image quantification. Finally, filter-based image analysis yields a label image (e.g., a binary segmentation mask), from which objects and object information yet need to be extracted. While this can be as straightforward as finding connected components, it can also be more sophisticated, like in *Largest Contour Segmentation* (LCS) (Manders et al, 1996) where multiple segmentations/objects are found for different thresholds and combined afterwards.

3.2 The machine-learning paradigm

The machine-learning approach is based on detecting patterns in numerical features computed from the image (reviewed by Shamir et al (2010)). This can mean classifying each pixel to be either part of an object, or not. However, the approach is not limited to pixels, and also patches and whole images can be classified, e.g., whether they contain cells or not. This classification is done based on features that are computed for each pixel or over the whole patch/image. The simplest feature is the (average) intensity. More advanced features include texture (Li et al, 2003; Orlov et al, 2008), gradients (Orlov et al, 2008), and shape (Etyngier et al, 2007). The machine-learning algorithm could, e.g., classify all bright regions with rough texture as belonging to a nucleus, or all images that contain curve-like shapes as images of filaments. Machine learning can also be used to classify spatial patterns without prior segmentation (Huang and Murphy, 2004). The machine-learning approach is frequently combined with the filter-based approach by either computing features of a filtered image where, for example, edges have been enhanced, or by computing features using filters.

Machine learning can follow either an unsupervised or a supervised approach (Cherkassky and Mulier, 1998; Duda et al, 2000; Bishop, 2007). In *unsupervised learning* the pixels/images are grouped according to their features using, e.g., clustering techniques. This yields "sub-populations" that have similar features within, but different ones across. Frequently, the assumption is that pixels or images of the same sub-population show the same type of objects, e.g., nuclei. In the *supervised* approach, the classification is learned from examples. The algorithm first has to be "trained" using pre-classified examples from each class. This typically means segmenting or classifying a number of images by hand in order to train the algorithm. The number of examples required for training depends on the number of features and the learning algorithm used. Prior knowledge is

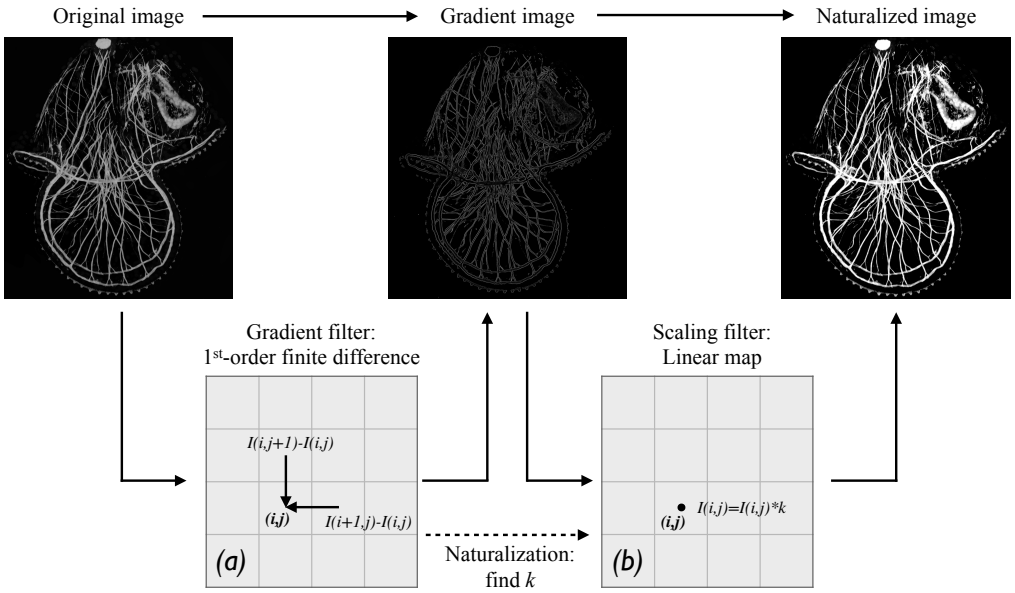

Figure 4: Example of a typical filter-based workflow: image naturalization for denoising and contrast enhancement (Gong and Sbalzarini, 2014). (a) The first filter computes the gradient of the input image by applying forward finite differences, subtracting each pixel intensity $I(i, j)$ from its top and right neighbors. (b) The second filter scales each pixel intensity by a value k that is automatically determined so that the naturalized image has a gradient histogram that fits the one expected from natural-scene images (Gong and Sbalzarini, 2014). (Original image from: American Microscopical Society, Winner of the 2004 Bauchsbaum Prize (amicros.org); Lee&Matus, U Hawaii, confocal image of *Pilidium* larva of the nemertean *Cerebratulus sp.*)

included both in the design of the learning algorithm and in the choice of features used for classification (Hong et al, 2008). Image information that is not captured by the selected set of features is lost. In the supervised approach, prior knowledge is additionally included in the training examples selected.

Machine learning is particularly popular for complex images, like electron microscopy images, MRI and X-ray images, and histological sections. In these images, texture and context often play an important role in detecting objects, hampering the design of generic filters or models. There, machine learning has for example been used to segment brain MRI images using supervised artificial neural networks (Reddick et al, 1997), to segment tumors in MRI images (Zhou et al, 2005), and to detect microcalcifications in mammograms (El-Naqa et al, 2002). Classification of image patches or whole images has, e.g., been used to classify sub-cellular patterns without previous cell segmentation (Huang and Murphy, 2004). This approach is particularly prevalent in histology (McCann et al, 2012) and pathology (Fuchs et al, 2008, 2009; Orlov et al, 2010), where entire images are often scored, e.g., for lymphoma detection (Orlov et al, 2010). This approach is illustrated in Fig. 5, where supervised classification of image patches is used to detect different tissue types, followed by classifying the overall histological score for the whole image. Frequently used image feature sets include *weighted neighbor distances* (WND) (Orlov et al, 2008), *scale-invariant features* (SIFT) (Lowe, 1999), *binarized statistical image features* (BSIF) (Kannala and Rahtu, 2012), and *basic image features* (BIF) (Crosier and Griffin, 2010). State-of-the-art supervised learning algorithms for image analysis include random forests (Breiman, 2001), regression tree fields (Jancsary et al, 2012), and deep neural networks ("deep learning") (Ciresan et al, 2012). Machine learning approaches to motion tracking started with using Support Vector Machines (Schölkopf and Smola, 2002), a popular supervised classification method, to track optical flows (Avidan, 2004). Later, this was generalized to *Relevance Vector Machines* that predict displacements rather than detecting flow, hence leading to a model-based Bayesian learning paradigm (Williams et al, 2005).

Machine-learning methods provide more flexibility than filter-based methods, albeit at the expense of higher computational time. Supervised approaches are particularly flexible, as they can be trained by example to solve a variety of image-analysis problems. Having to manually annotate and select the training samples, however, is additional effort. Moreover, the final analysis depends on the chosen training data, hence introducing additional user bias that is not present in other methods. Usually, one wishes to keep the feature set as small as possible, as the computational cost of machine-learning algorithms grows with the number of features used. In a supervised

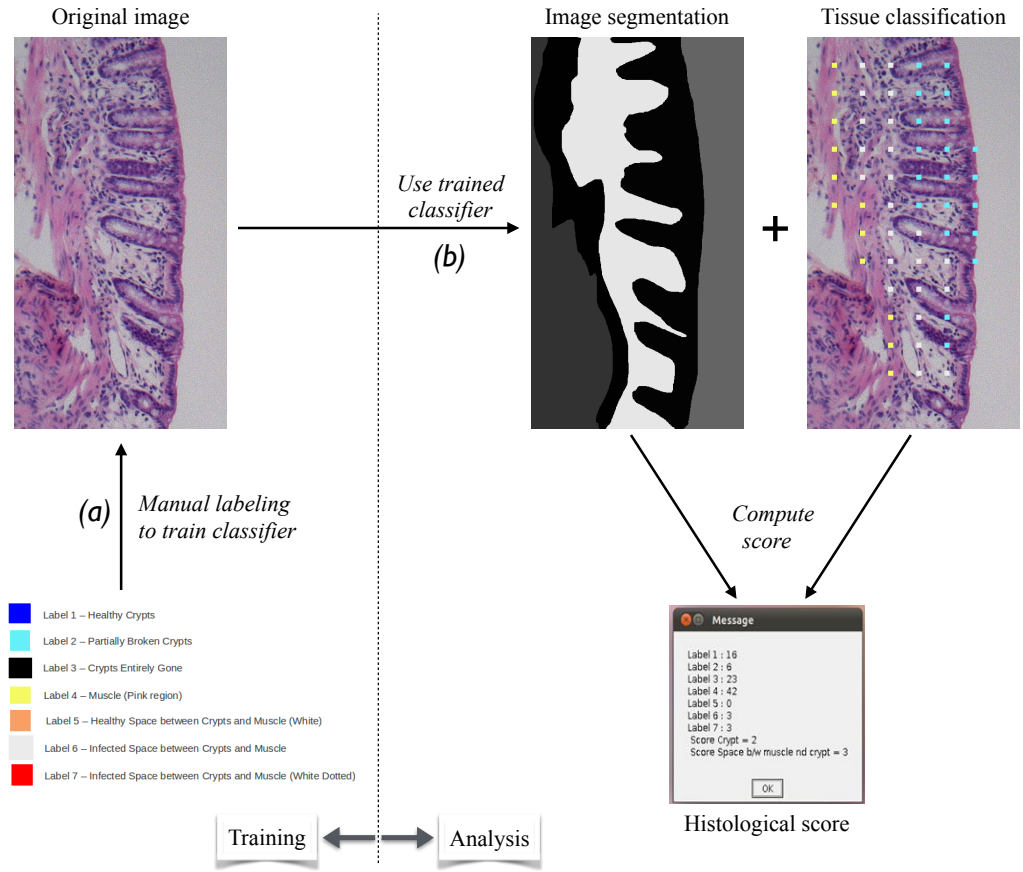

Figure 5: Example of a typical machine-learning workflow: automatic scoring of histology sections for colitis detection. (a) The machine-learning classifier is trained by the user manually labeling the tissues in several example locations. (b) After training, the classifier can be used to segment the image and automatically assign tissue class labels everywhere. From these, the final histological score is computed. The example shown here uses the Random Forest classifier from *WEKA* (Hall et al, 2009) on the *WND-CHARM* (Orlov et al, 2008) image features. Prior to training, 22 out of the 1025 features were determined to be important for the problem (feature selection). (Original image from: Institute of Physiology, University Hospital Zurich, mouse colitis histology section; Segmentation and classification by Dheeraj Mundhra, MOSAIC Group.)

approach, the amount of training data needed also increases with the feature count. Deciding which features to include is a hard problem known as *feature selection*. Finally, like in filter-based approaches, pixel-level classification yields a labeled output image from which objects and their properties still need to be extracted. This image-to-object transformation implies additional prior knowledge and can also be done using machine learning.

3.3 The model-based paradigm

The model-based approach does not operate on the pixels of the observed image, but rather estimates a model of the imaged scenery that is most likely to explain the observed image. The image is hence only used as a gold standard to compare with. A key ingredient is *how* a hypothetical segmentation or scenery is compared with the image, and how the result of this comparison is used to iteratively refine and improve the former. Approaches range from comparing image intensities (Kass et al, 1988) or gradients (Lin et al, 2003) to including a predictive model of the image formation process (Helmuth et al, 2009). The latter is illustrated in Fig. 6, where the segmentation is iteratively updated until the output of the forward problem (see Sec. 2.2) fits the observed image as closely as possible.

Model-based image analysis requires up to three models to be specified: the object model, the imaging model, and the noise model. In many cases, not all three are present, or some are implicitly assumed to be, e.g., the identity map or a Gaussian. The *imaging model* describes the noise-free image-formation process, predicting the

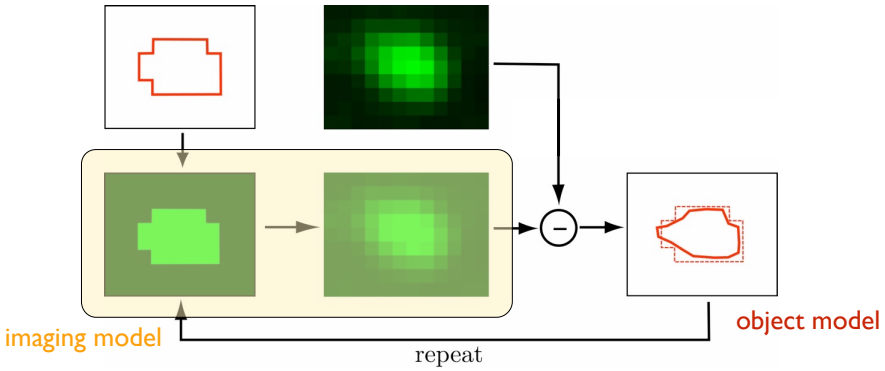

Figure 6: The model-based approach: an imaging model is used to predict the expected image for a given, hypothetical segmentation. This predicted image is then compared with the actually observed image and the segmentation is adjusted to minimize the difference between the two. The specific metric used to quantify the difference implicitly defines the noise model one assumes. The object model defines what shapes, deformation, and intensity distributions are admissible for the segmentation (Credit: Jo Helmuth, MOSAIC Group).

image one would *expect* (over the statistical distribution of the noise) to see when imaging a particular scenery. A simple imaging model for a fluorescence microscope is the convolution with the PSF (Linfoot and Wolf, 1956; Zhang et al, 2007), neglecting any noise. For phase-contrast microscopy, the imaging model is more complex (Yin et al, 2010). If the image-formation process is not to be accounted for, the imaging model can also be the identity map. If the comparison is not done on pixel intensities, but on other features, such as intensity gradients, the imaging model computes these features (Lin et al, 2003). The hypothetical sceneries that are scored by the imaging model correspond to different realizations of the object model. The *object model* defines the admissible sceneries and parameterizes them. A simple object model for a nucleus could be a sphere, parameterized by its center location and radius. For each realization of this model, i.e., concrete values for center and radius, the imaging model predicts how the image features of that nucleus would look like (e.g., bright spot around the projection of the sphere with some diffraction blur at the boundary). The imaging and object models can be arbitrarily complex and may even include physics-based numerical simulations. For example, segmenting cardiac deformation from ultrasound images has been done using a finite-element simulation of the mechanics of the myocardium as an object model (Papademetris et al, 1999). Finally, the *noise model* specifies the statistical distribution of the imaging noise, hence providing statistical significance to the comparison between imaging model and data. In the simplest case, the noise model defines how to compare the imaging-model output with the image data (Paul et al, 2013). Assuming Gaussian noise on the data, one would for example compare images by the sum of squared pixel-intensity differences. Other noise models lead to different comparison metrics (Chesnaud et al, 1999; Martin et al, 2004; Paul et al, 2013). In many cases, the noise model is not explicit, but implicitly assumed, e.g., in the way the imaging model is evaluated, or in the features of the image used for the comparison.

Model-based approaches are mostly classified with respect to the model assumptions. Examples include piecewise constant object models that assume the intensity within each object to be uniform (Fig. 7). Piecewise smooth object models allow for intensity gradients within an object (Fig. 8). Deconvolving imaging models account for the PSF of the microscope (Fig. 7). Data-driven models try to fit features (e.g., gradients) learned from data. A second classification is with respect to the algorithm used to determine the best scenery. Examples include statistical estimators (Zhu and Yuille, 1996), variational solvers (Chan and Shen, 2005), sampling schemes and random fields (Geman and Geman, 1984), combinatorial optimizers (Blake et al, 2011), graph-based optimizers (Boykov et al, 2001), dynamic programming (Nilufar and Perkins, 2014), and greedy gradient descent (Kass et al, 1988).

A dynamic-programing approach was, for example, used for whisker tracing (filament segmentation) in behavioral videos of mice, by Bayesian inference over a whisker object model (called "detector" therein) (Clack et al, 2012). Additionally including an imaging model, model-based image analysis has been used to determine deconvolved segmentations without computing a deconvolution (Helmuth and Sbalzarini, 2009; Helmuth et al, 2009). Because the imaging model accounts for PSF blur and imaging noise, the segmentations in Fig. 7 jointly solve the deconvolution and segmentation tasks (Paul et al, 2011, 2013). This is beneficial when segmenting small objects near the diffraction limit, like the Rab5-GFP endosome domains in Fig. 7. The model-based approach

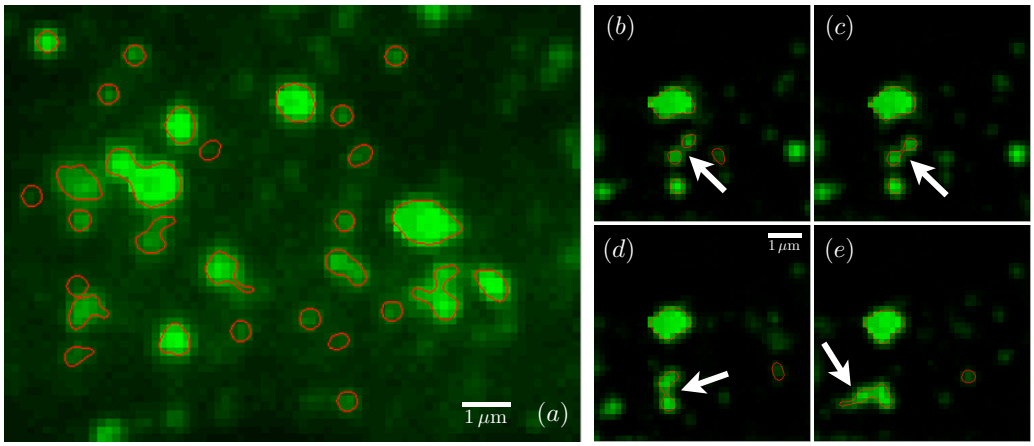

Figure 7: Example of model-based image segmentation, accounting for the Point Spread Function (PSF) of the microscope to get high-resolution outlines of small intracellular objects (Helmuth et al, 2009; Helmuth and Sbalzarini, 2009). The images show maximum-intensity projections of confocal z-stacks of fluorescently labeled Rab5, a protein localizing to endosomes. (a) The red outlines show the resulting object boundaries using deconcolving active contour segmentation (Helmuth et al, 2009; Helmuth and Sbalzarini, 2009). (b)–(e) Time-lapse sequence of reconstructed Rab5–GFP outlines illustrating a fusion event (arrow). (raw images: Greber lab, University of Zurich; segmentations: Jo Helmuth, MOSAIC Group.)

also allows including physical properties of the imaged objects, such as bending stiffnesses of lipid membranes, hence ensuring that the image-analysis result corresponds to a physically feasible membrane configuration. This can be useful, e.g., when studying cell-edge dynamics in polarizing and migrating keratocytes (Ambühl et al, 2012). Efficient 3D methods for model-based image segmentation are also available (Boykov et al, 2001; El-Zehiry and Elmaghraby, 2009; Cardinale et al, 2012) and topological constraints on the objects can be accounted for (Cardinale et al, 2012) (Fig. 8). Data-driven models have been used to robustly segment dense and touching nuclei in fluorescence microscopy images using a gradient model (Lin et al, 2003).

Model-based approaches are also popular for motion tracking (Kalaidzidis, 2007, 2009), for example based on a model of how the objects move (Crocker and Grier, 1996), using approximate graph matching to fit a model to the data (Vallotton et al, 2003), using approximate combinatorial optimization methods for model fitting (Sbalzarini and Koumoutsakos, 2005; Ruhnow et al, 2011; Jaqaman et al, 2008), using Kalman filters based on linear state-space models (Li et al, 2006, 2007), using particle filters based on non-linear state-space models (Hue et al, 2002; Smal et al, 2008; Cardinale et al, 2009), using Bayesian probabilistic models for multi-target tracking (Genovesio and Olivo-Marin, 2004) and multiple hypothesis tracking (Cox and Hingorani, 1996), and using integer-programming optimization over graph-based motion and appearance models (factor graphs) (Schiegg et al, 2013).

Model-based image analysis includes prior knowledge via the imaging, noise, and object models. While only the latter constitutes a prior in the Bayesian sense, all encode prior knowledge. Postulating the wrong models leads to wrong results. Therefore, the model-based approach is particularly suited to clear-cut cases, like fluorescence microscopy, where the object and imaging models are suggested by physics. However, even when using appropriate models, the resulting optimization problem can be difficult to solve and is often restricted to local optimization starting from a user-specified initial segmentation (Kass et al, 1988; Helmuth et al, 2009; Helmuth and Sbalzarini, 2009; Cardinale et al, 2012) (Fig. 8). This is relaxed in globally optimal methods, which are independent of initialization and guarantee that there is no other result that would explain the image better than the one found (Pock et al, 2009; Brown et al, 2011; Paul et al, 2011, 2013). While this result may still be wrong, it uses all the information available in the image and represents the best-possible result under the assumed models (Rizk et al, 2014). This is a strong statement that is much harder to make in the filter and machine-learning paradigms. Another important advantage of model-based methods is that they are physics-based and the same algorithm can be used for a variety of cases by swapping the model. Switching from fluorescence to phase-contrast images can be as easy as replacing the imaging model accordingly, leaving the algorithm unchanged. Finally, model-based approaches directly yield objects and object properties. They hence unite image labeling and image-to-object transformation into a single step.

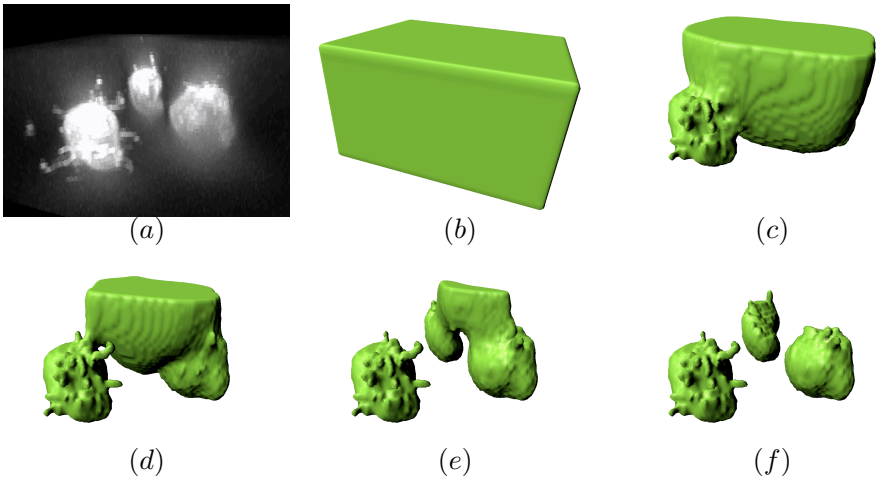

Figure 8: 3D model-based segmentation of germ cells in a zebrafish embryo. (a) The raw 3D confocal image stack, showing three cells with a fluorescent membrane staining. The intensity is inhomogeneous, with the background over the top of the cells brighter than the interior at the bottom of the cells. (b) Initial segmentation provided by the user to the algorithm from Cardinale et al (2012). (c)–(f) Evolution of the outline as computed by the algorithm, converging to the final segmentation using a piecewise smooth object model and a fluorescence imaging model. (Raw image: Mohammad Goudarzi, University of Münster; segmentations: Janick Cardinale, MOSAIC Group.)

4 Challenges in computational bio-image analysis

There are currently four major challenges in computational bio-image analysis: large and multidimensional data, uncertainty quantification, more generic algorithms, and collaborative open-source software. In addition, there are several challenges in related areas, such as image databases (Swedlow et al, 2003), annotation systems (Peng et al, 2010), and gold standards for testing and benchmarking of algorithms (Rajaram et al, 2012; Vebjorn et al, 2012). Together with the advancements in optics, microscopy, and labeling techniques, these developments will enable unprecedented image-based studies.

4.1 Large and multi-dimensional data

In bio-image analysis, big data comes in two flavors: many images or large images. The former is typically the case in high-throughput screens (Collinet et al, 2010) and can be dealt with by distributing the images over multiple computers for analysis. The latter is a feature of multi-dimensional and high-resolution imaging techniques, such as imaging mass spectrometry (Stoeckli et al, 2001) and light-sheet microscopy (Huisken et al, 2004; Engelbrecht and Stelzer, 2006) and requires solutions within a single image. This can, for example, be done by multi-scale image representations, such as scale-space approaches (Witkin, 1984) and super-pixels (Xu and Corso, 2012), akin to the "Google Maps" zooming function.

However, the question arises as to what should be done if the imaging equipment delivers data at a faster rate than what can be written to hard disks. Recent microscopes with CMOS cameras, for example, deliver 3D images at a rate of 1 GB/second, per camera. A setup that uses two cameras hence produces almost 173 TB of data a day (Reynaud et al, 2014). This is faster than any hard disk or other permanent storage system could archive the images and raises data-handling and storage issues that have so far been confined to the high-performance computing and particle physics communities (Tomer et al, 2012; Weber and Huisken, 2012). Storing all raw images that come from such microscopes is infeasible. Using lossless data compression techniques, however, fast networks are able to stream the data directly into a computer cluster, where it can be distributed across multiple computers for analysis. Only the analysis results are then stored, e.g., the positions of all nuclei or the shapes, sizes, and locations of all cells in the tissue. If the analysis is to be repeated, it is quicker to image another sample than to archive the raw data, read it back, and re-run the analysis. This trend is also observed in large computer simulations running on supercomputing systems and is known there as the "data gap" (Sbalzarini, 2010). Analysis results and visualizations are hence determined at runtime, and if later a new variable is to be measured or a new feature to be computed, the whole simulation is re-run.

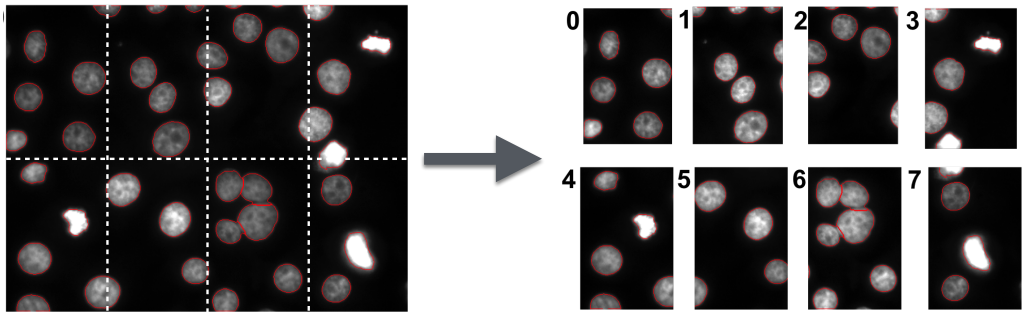

Figure 9: Domain-decomposition approach to deal with big image data as presented by Afshar and Sbalzarini (2016). A large image is subdivided into several smaller sub-images that are each given to a different computer or cluster node for processing. The different computers (0 to 7 in this example) communicate with each other over the network whenever segmentations cross sub-image boundaries. This ensures that the overall segmentation is the same as that which would have been obtained on a single computer. The distributed result, however, is computed faster (here: about 8 times faster) and using less memory on each computer. (Raw image: Dr. Liberali, University of Zurich; distributed segmentation by Yaser Afshar, MOSAIC Group.)

Not storing the raw data comes with two requirements: (1) The analysis software needs to run in real time, possibly distributed across multiple computers. (2) The confidence intervals and uncertainties of the analysis results need to be known and stored along with the results.

The first requirement is of technical nature. Individual computer processor cores are not getting faster any more at the rate they used to. Instead, chip manufacturers pack multiple cores into each processor and have them operate in parallel. Leveraging this speedup, however, requires that algorithms are designed and implemented with parallelism in mind. This is often not straightforward and requires re-thinking many image-analysis algorithms. One way that is currently uncommon is to distribute each image (Afshar and Sbalzarini, 2016). Instead of having one processor core analyze image after image, the images are divided into smaller sub-images that are scattered across multiple cores (see Fig. 9). Each core then works on its part of the image and they exchange information with the other cores over a computer network in order to collectively solve the global analysis task in a fraction of the time it would take a single core to do so (Nicolescu and Jonker, 2000). This requires image-analysis algorithms that can be divided into concurrent work packages with as little interdependencies as possible (Seinstra et al, 2002). Every interdependence between work packages causes network communication overhead, which keeps the involved processor cores from working during that time. Modern computer hardware, such as graphics processing units (GPUs) and heterogeneous many-core processors, have more than a thousand parallel cores that need to be kept busy and orchestrated. It is hence essential that we develop algorithms that map well onto such computer architectures (Galizia et al, 2015), like the example of motion tracking using parallel distributed particle filters (Demirel et al, 2014a) implemented using the PPF software library (Demirel et al, 2014c), and parallel distributed image segmentation (Afshar and Sbalzarini, 2016).

The second requirement when not storing the raw data is uncertainty quantification. If one only stores the analysis results, but not the raw images, it is impossible to later go back and check whether there really was a nucleus in that strange outlier image, or not. We would never know how much of the data is noise, and what is signal. Storing proper confidence intervals would, however, tell us that the probability that there actually was a nucleus is, e.g., 10%. So we know that the data point is not to be trusted, because the algorithm was not sure about what it "sees" in that image. Storing the analysis results with their associated uncertainties enables statistical significance tests in order to decide whether an observed difference between samples is real, or not. This links to the challenge of uncertainty quantification.

4.2 Uncertainty quantification

The previous example describes a situation where uncertainty quantification is indispensable. However, it is useful in far more cases. An algorithm for segmenting cells in a tissue could, for example, automatically detect regions in the image where it cannot determine a confident segmentation and flag the user to look specifically at those regions when manually post-processing the result. This would greatly reduce the proofreading overhead.

One could then also specify a confidence level and instruct the algorithm to only flag cases where the result is less than, say, 95% likely to be correct. If a mutant or knock-down then shows less than 5% difference in the readout, we know that this is not significant and could as well be explained by image-analysis errors. Clearly, uncertainty quantification is desirable and useful.

Unfortunately, uncertainty quantification is a hard problem and has therefore not received much attention in image analysis so far. It is often difficult to express uncertainty "scores" as true probabilities, because the normalization is unknown. Evidence theory (Shafer, 1976) could hence provide a more straightforward way of expressing uncertainty (see Sec. 2.3). Regardless of their expression and interpretation, however, uncertainties in biological image analysis mainly arise from three sources:

1. The noise in the raw image is propagated through the computational analysis pipeline, leading to (potentially amplified) noise and uncertainty in the analysis result.
2. The algorithm may terminate with a solution that is not the best possible one, leaving some uncertainty about how far from the best solution it is.
3. The prior knowledge on which the algorithm is based may not adequately describe reality, leading to uncertainty about how much of the result is due to this inadequacy.

Source (1) is particularly prevalent in fluorescence microscopy, where the imaging noise is often significant. This noise may be further amplified by the image analysis. Consider, e.g., an edge detector that computes differences between pixels, or a watershed filter that compares which of two pixels is brighter. If both pixel intensities are noisy to within $\pm 10\%$, the difference is noisy to within $\pm 20\%$ and the watershed may go down the wrong way. The noise is hence amplified, leading to results that are less reliable than the original data. A famous example of a noise-amplifying process is deconvolution. Source (2) is mostly important in machine-learning and model-based methods, were the final estimated classification or scenery may not be the *global* optimum over *all* possibilities, but only a local optimum over a subset of tested possibilities. Source (3) is again relevant to all three paradigms, since all of them include prior knowledge in the filter design, feature selection, or model specification that could be wrong or inadequate.

Ideally, we quantify the uncertainty in the final result due to the combined effects of all three sources, or at least provide an upper bound for it. Unfortunately, this problem is hard (Halpern, 2005). Ground truth is not available, synthetic benchmark images frequently do not share the intricacies of real images, a theoretical framework for inference over images is lacking, and theoretical performance guarantees are not available for many algorithms. Nevertheless, several promising approaches can be identified.

The first approach includes efforts to generate hand-segmented benchmark image collections (Vebjorn et al, 2012). The accuracy and robustness of algorithms can be tested on these image collections and scored against the manual gold standard. This approach works as long as the images that the algorithms are later going to be applied to are similar to the benchmark images. Since they are not going to be exactly the same, though, this introduces uncertainty about the uncertainty quantification. Moreover, the manual gold standard is not free of human error. Both points are somewhat relaxed by using synthetic ground truth (Rajaram et al, 2012). There, ground truth is known without uncertainty, and the forward model used to generate the synthetic images can be adapted to different acquisition conditions. The key difficulty, however, is to provide sufficiently realistic (in shape, noise distribution, fluorophore blinking etc.) ground truth and forward models. Using inappropriate models again leads to uncertainty in the uncertainty estimate, according to source (3) above. Realistic shapes can, for example, be generated by sampling from shape spaces learned from training images (Murphy, 2012). This, however, introduces uncertainty with respect to the training data chosen for learning the shape space.

The above approaches to uncertainty quantification are data-centric. There are, however, also algorithm-centric approaches that relax the data dependency to some extent. Source (1) can, for example, be addressed by error-propagation analysis of the involved algorithms. The conceptual idea is to re-run the analysis for different random input perturbations and see how the results vary. This is commonplace in scientific computing, where a wealth of efficient methods has been developed, including spectral uncertainty quantification (Le Maître and Knio, 2010), simplex stochastic collocation (Witteveen and Iaccarino, 2012), and generalized polynomial chaos expansion (Xiu and Karniadakis, 2002; Xiu, 2009). However, these are still rarely used in image analysis, with exceptions like *OMEGA*, which uses error propagation in particle-tracking analysis (https://github.com/OmegaProject).

Most algorithm-centric approaches so far have focused on source (2) by quantifying the residual discrepancy between the model output and the real image. These approaches do not require ground truth, but rather measure model-fitting errors. They hence only provide a *lower* bound on the real uncertainty and usually do not yield proper probabilities, but rather evidence (Shafer, 1976). The simplest approach is to use the residual value of the posterior probability as a proxy for result certainty (Paul et al, 2013) (Fig. 10a). More sophisticated approaches use Markov-chain Monte Carlo sampling (Geman and Geman, 1984; Chang and Fisher III, 2011) or Approximate Bayesian Computation (Marjoram et al, 2003) to sample from the probability density of the posterior and get an idea of the distribution of potential results. This has, e.g., been used to provide uncertainty estimates in microtubule tracking (Cardinale et al, 2009) (Fig. 10b), model-based segmentation (Cardinale, 2013) (Fig. 10c), and multi-scale approaches (Kohli et al, 2010). In addition, theoretical performance guarantees are available for some optimizers and estimators used in model-based methods. Examples include graph cuts (Boykov et al, 2001), Markov random fields (Geman and Geman, 1984), and photometric estimators based on information theory (Paul et al, 2013). While these error bounds do not provide a probability distribution, they give an idea of the interval within which the correct result must lie. These intervals, however, are in the model-fitting energy and not in object space. If the energy is flat (i.e., has a small gradient), the result might be arbitrarily wrong and still have similar energy. This problem is addressed by the concept of *diversity solutions*, which are alternative segmentations or analysis results that are all about equally likely to be true, but may look very different (Ramakrishna and Batra, 2012; Batra et al, 2012). Using diversity solutions, a segmentation algorithm could for example express its uncertainty about two overlapping blobs of high intensity being two individual touching objects, or one fused object. Ideally, globally optimal methods are guaranteed to find the best solution and are hence free of source-(2) uncertainty (Pock et al, 2009; Brown et al, 2011). This, however, is only possible for simple object and imaging models, trading off uncertainties of source (3).

Source (3) is a classic issue in machine learning, called *model misspecification error*. To our knowledge, it has so far not been addressed in image analysis. One way to do so could be to combine machine-learning and model-based methods on the same problem. Looking at the discrepancy between the results could provide an estimate of how much uncertainty is explicable by modeling errors.

Finally, rather than asking how well a given algorithm performs on an image, one could ask how well *any* algorithm could *possibly* perform. For example, with what uncertainty is one able to quantify the center of a point source from a fluorescence microscopy image given the finite number of photons recorded? These are questions about absolute, often information-theoretic, bounds. For point localization, the problem has been solved using the concept of Cramér-Rao bounds, providing a lower bound on the estimation error any algorithm must necessarily make, given the photon count (Ober et al, 2015). For higher-dimensional objects, such as filaments, areas, and volumes, the situation is considerably more complex, since neighboring photon sources are correlated though the (unknown) geometry of the object. For filaments, bounds have been derived for specific cases Xiao et al (2016), but for two- and three-dimensional objects nothing is available yet.

4.3 Generic algorithms

A current shortcoming in bio-image analysis is the tendency to treat every problem as a special case and develop a new algorithm or software for each project, to solve exactly the specific problem of that project. While this case-by-case approach and the associated "whatever works" mentality mostly lead to the desired results, they are wasteful and not scalable. Not only does it take a long time to come up with and implement a new analysis algorithm, it is a recipe for reinventing the wheel. Research groups hire image-processing specialists and computer programmers that often reinvent or re-implement what was already there in another group, and central image-processing facilities (if existent at all) drown in unrelated requests and do not find time to provide more general, unifying solutions. One of the most precious features of an algorithm is its generality. A strong trend in the field hence goes toward developing and implementing algorithms that are more generic and that are applicable to more than just one case or imaging modality. This also includes collections of canned algorithm building blocks and software libraries that can be used by computer programmers to more rapidly build workflow solutions from proven components (see also Sec. 4.4).

On the algorithmic level, there are three main axes of generality: (1) combining multiple tasks into one, (2) extending the class of problems that a given algorithm can deal with, (3) rendering an algorithm parameter-free.

The first point could, e.g., include combining image restoration with segmentation and photometry. An example

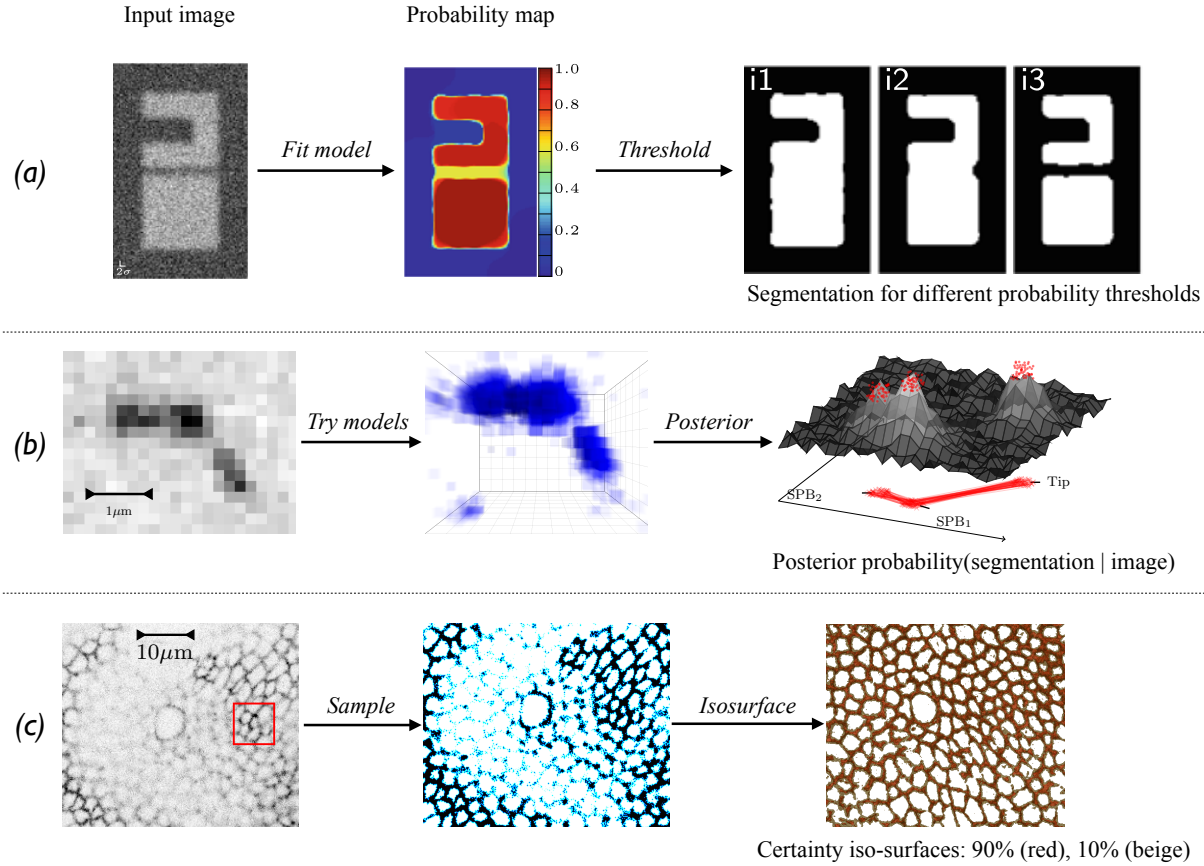

Figure 10: Approaches to uncertainty quantification in image analysis. In all approaches, the input image (left) is first transformed to a probability or evidence map, from which the result is then computed. (a) In the approach of Paul et al (2013), the residual of a globally optimal model fit is used to estimate a probability map for each pixel to be part of an object. Thresholding this map at different probability cutoffs gives different alternative segmentations for different confidence levels (i1–i3). (b) The approach of Cardinale et al (2009) applied to tracking microtubule tips using particle filters (Demirel et al, 2014b). The particle filter tries many different possible model fits in order to form a cloud of possible tip localizations (middle). Using the resulting particle representation of the posterior (Demirel et al, 2014b), the most likely tip positions and their variances can be extracted. (c) The approach of Cardinale (2013) uses Markov-chain Monte Carlo sampling to sample many possible segmentations from the model posterior. This yields an unnormalized evidence map (darker means higher evidence) from which iso-surfaces can be computed. These iso-surfaces contain the correct segmentation with the indicated evidence. (Image sources: input image in (a) from Grégory Paul, MOSAIC Group, synthetic test image; input image in (b) from Barral lab, ETH Zurich, fluorescently labeled spindle-pole bodies (SPB) and spindle tip in dividing *S. cerevisiae*; input image in (c) from Basler lab, University of Zurich, fluorescently labeled membranes in a *D. melanogaster* wing imaginal disc; result in (a) by Grégory Paul, MOSAIC Group; results in (b) and (c) by Janick Cardinale, MOSAIC Group.)

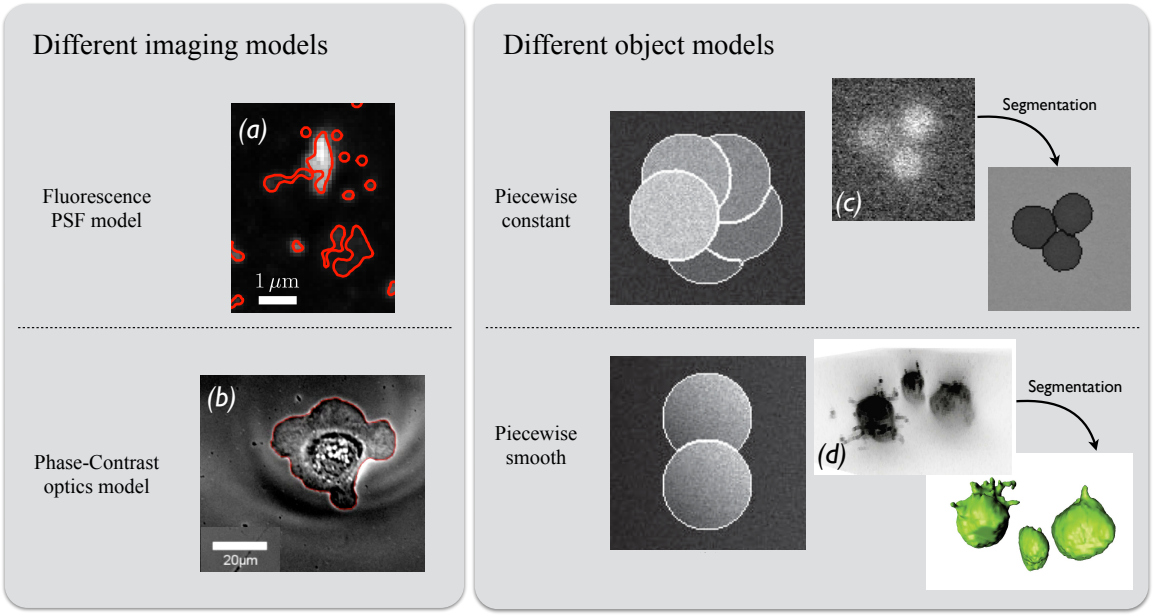

Figure 11: Flexibility of model-based analysis by replacing the model in the same algorithm. Left: The model-based Snake method (Kass et al, 1988) can be used to segment (a) fluorescence images of Rab5-EGFP endosomes in HER911 cells (Helmuth and Sbalzarini, 2009), as well as (b) phase-contrast images of polarizing fish epidermal keratocytes (Ambühl et al, 2012) by changing the imaging model. Changing the object model allows segmenting piecewise constant or piecewise smooth objects (Cardinale et al, 2012), such as (c) fluorescently labeled cells with cell-specific uniform staining (Cardinale, 2013) and (d) fluorescently labeled zebrafish primordial germ cells with highly non-uniform signal (Cardinale et al, 2012). The synthetic "ice-cream" images illustrate the concept of piecewise constant and piecewise smooth object intensities. (Image sources: raw image in (a) from Greber lab, University of Zurich; raw image in (b) from Verkhovsky lab, EPFL; raw image in (c) from BCS Group, TU Darmstadt; raw image in (d) from Mohammad Goudarzi, University of Münster; segmentation in (a) by Jo Helmuth, MOSAIC Group; segmentation in (b) by Mark Ambühl, Verkhovsky lab, EPFL; ice-cream images and all segmentations in (c) and (d) by Janick Cardinale, MOSAIC Group.)

are deconvolving active contours (Helmuth and Sbalzarini, 2009) (see Fig. 7) that combine image deconvolution with segmentation by directly providing segmentation results that are compatible with the microscope's PSF. Along the same lines, image denoising, deblurring, and segmentation have been combined into a single step using the concept of Sobolev gradients (Jung et al, 2009). Segmentation has also been combined with denoising, deconvolution, and inpainting into a single level-set or split-Bregman model-based algorithm (Paul et al, 2013, 2011), as implemented in the Squassh plugin for *Fiji* and *ImageJ* (Rizk et al, 2014). Jointly solving the image restoration (e.g., denoising, deconvolution, dehazing, inpainting) and segmentation problems leads to better results than doing so sequentially (Paul et al, 2013). The reason is that while both individual problems are ill-posed, they naturally regularize each other when considered jointly. Computing a deconvolution, e.g., is ill-posed because there is a multitude of results that map to the same image when convolved with the microscope PSF. The result is hence not unique, and depending on how the parameters of the deconvolution algorithm are tuned, different results can be obtained. When segmenting at the same time, however, the deconvolution method does not have to produce a complete image, but only has to work in the limited solution space of segmentations. Since this space is smaller, the ambiguity is reduced.

The second point is mostly addressed by machine-learning or model-based frameworks. Both provide principled ways of adapting to new situations. This is less obvious in filter-based methods, where the problem-specific prior knowledge is implicitly included in the filter design. Changing to a new problem (e.g., from segmenting fluorescence images to segmenting phase-contrast images) would require one to re-design the filter. Machine-learning and model-based frameworks "externalize" the prior knowledge and allow one to change it without changing the core of the algorithm. In machine learning, this may be as simple as re-training the algorithm using a new set of training images (e.g., phase-contrast instead of fluorescence). In a model-based approach, the object model and/or imaging model can be replaced to adapt the algorithm to different problems. This is illustrated in Fig. 11.

The third point aims at rendering algorithms parameter free. Most image-analysis algorithms have a number of user-adjustable parameters. Only few algorithms work across a spectrum of problems without requiring parameter tuning. These parameter-free algorithms are particularly popular because they are easy to use and deliver robust performance across many applications. Examples include Otsu thresholding (Otsu, 1975) and image naturalization (Gong and Sbalzarini, 2014). There is a clear trend in the field to reduce the number of parameters of an algorithm with the ideal goal of rendering it more versatile and easier to use.

4.4 Collaborative open-source software

In addition to providing generic and flexible algorithms, another proven remedy against reinventing or re-implementing existing methods is to share software and create public repositories of open software modules. This motivates the trend for creating and maintaining collaborative open-source software for bio-image informatics (Swedlow and Eliceiri, 2009). However, the need for open-source development reaches deeper than merely alleviating the implementation overhead for new projects. It is a fundamental prerequisite for reproducible science. Closed-source software is a black box that often does not provide enough information about the algorithms implemented. Open-source software is one way of rendering image analysis transparent, but its coordinated development and long-term maintenance come with their own set of challenges, in particular with respect to project coordination and funding (Cardona and Tomancak, 2012).

Open-source software is frequently developed in academic labs by scientists who are not professional software engineers. This has traditionally had a negative effect on the usability and user-friendliness of such software. While guidelines for software usability are available, enforcing them remains challenging (Carpenter et al, 2012). Open-source projects also frequently start as individual research projects with specific biological questions in mind. Many pieces of software organically grew from there, becoming more and more generic, but the original application they were conceived for often remains the focus of the software. While this provides a rich landscape of software tools and libraries (Eliceiri et al, 2012), each with a specific application niche, it also raises the question of how integration and interoperability between the various tools can be achieved. Data exchange between different tools and pipelining of tools are the main challenges for the developer community in the coming years.

From a user-interface point of view, four different design philosophies can be distinguished, as illustrated in Fig. 12: The first is to provide a general-purpose command-line or scripting language with a large collection of toolboxes and subroutines that the user can combine for image analysis. This is the approach taken by tools like *R*, *Octave* (an open-source *MATLAB* look-alike), *ScyPi*, and *PIL*. These tools are particularly flexible and generic, are well suited for batch processing of large image collections, but require the user to have basic scripting skills. A second design philosophy is to provide an interactive graphical user interface, mostly combined with a plug-in architecture for third-party developers to contribute their algorithms. Examples include *ImageJ* (Abramoff et al, 2004; Schneider et al, 2012), *Fiji* (Schindelin, 2008; Schindelin et al, 2012), *Icy* (de Chaumont et al, 2011, 2012), *Vaa3D* (Peng et al, 2010, 2014), *bisque* (Kvilekval et al, 2010), *OMERO* (Swedlow and Eliceiri, 2009), *FARSIGHT* (Roysam et al, 2008), *CellCognition* (Held et al, 2010), *MorphoGraphX* (Barbier de Reuille et al, 2015), and *BioImageXD* (Kankaanpää et al, 2012). A third design approach puts the analysis workflow center stage, frequently specified using a graphical data-flow language. Examples of this kind are *CellProfiler* (Carpenter et al, 2006; Lamprecht et al, 2007), the workflow engine *KNIME* (Berthold et al, 2008), the workflow engine *LONI Pipeline* (Rex et al, 2003) and the image-processing environment *MiPipeline* (Nandy, 2015) based thereon, and the image-processing environment *Anima* (Rantanen et al, 2014) based on the workflow engine *ANDURIL* (Ovaska et al, 2010). The fourth approach is to implement large collections of generic image-analysis algorithms in well-tested software libraries that provide an API for developing user programs. This is the most generic approach, but requires the user to have programming skills. Popular examples include the libraries *ITK* (Ibanez et al, 2005) and *VIGRA* (Köthe, 1999) for image analysis and processing, *OpenCV* (Bradski and Kaehler, 2008) for computer vision, and *OpenGM* (Andres et al, 2012) for machine learning.

Virtually all of these software projects implement filter-based analysis. However, many have their own specialization. *ImageJ* (Abramoff et al, 2004; Schneider et al, 2012) is, for example, particularly well suited for 2D microscopy image analysis. *CellCognition* (Held et al, 2010) caters to time-lapse cell culture imaging, *CellProfiler* (Carpenter et al, 2006; Lamprecht et al, 2007) was originally developed for image-based high-throughput screens (Snijder et al, 2009), *MorphoGraphX* (Barbier de Reuille et al, 2015) originated as a tool for plant tissue

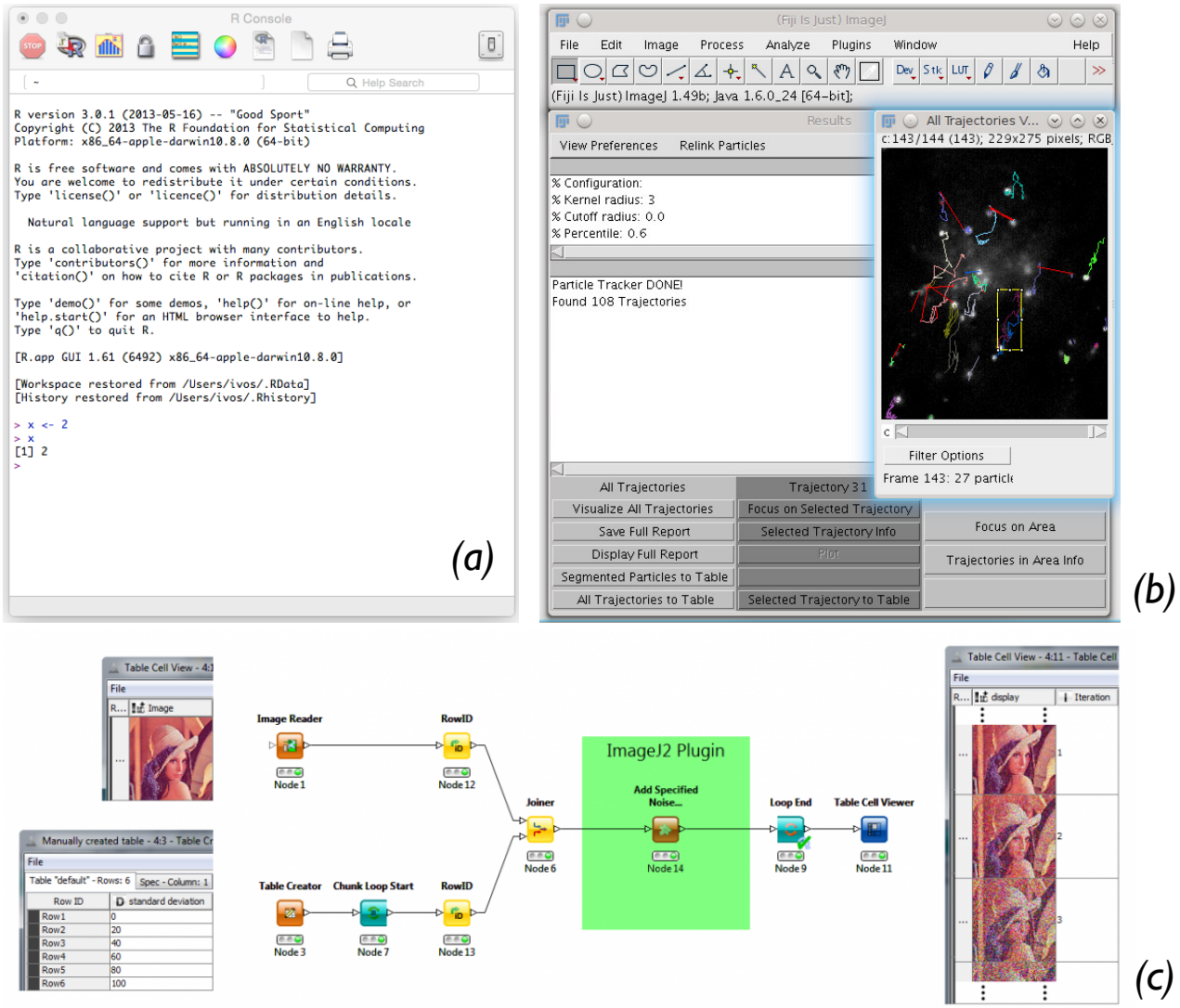

Figure 12: Different user-interface philosophies. (a) The scripting interface of *R* offers access to thousands of functions, but requires scripting skills. (b) The point-and-click graphical user interface of *Fiji* (Schindelin, 2008; Schindelin et al, 2012) requires no programming skills, but offers limited flexibility. (c) The workflow design interface of *KNIME* (Berthold et al, 2008), showing a workflow for image processing with an *ImageJ2*-plugin integrated. This approach requires programmatic thinking and offers intermediate flexibility. (Image credits: (a) and (b) own screenshots; (c) from knime.org)

morphogenesis, *Vaa3D* (Peng et al, 2010, 2014) and *BioImageXD* (Kankaanpää et al, 2012) started as interactive 3D visualization tools and are particularly strong at big image data visualization, and *bisque* (Kvilekval et al, 2010) and *OMERO* (Swedlow and Eliceiri, 2009) have their particular strength in primarily being image databases. In addition to these generic tools, there are many specialized and often application-specific tools available, such as *PackingAnalyzer* (Farhadifar et al, 2007; Aigouy et al, 2010) to segment cell membranes in developing epithelial tissues with fluorescent membrane staining, *FIESTA* (Ruhnow et al, 2011) to segment fluorescently labeled filaments, and *OMEGA* (https://github.com/OmegaProject) for virus particle tracking with uncertainty quantification.

Software packages specifically supporting model-based image analysis include *Icy* (de Chaumont et al, 2011, 2012) for fluorescence microscopy images and *itk-SNAP* (Yushkevich et al, 2006) for medical images. The *BioImageSuite* (Duncan et al, 2004) supports model-based image segmentation using Markov random fields (Geman and Geman, 1984). The *FARSIGHT* toolkit (Roysam et al, 2008) and *BioImageXD* (Kankaanpää et al, 2012) make available several model-based methods from the *ITK* library (Ibanez et al, 2005). Model-based image analysis plug-ins are also available for *ImageJ* (Kaynig et al, 2010) and *bisque* (Bertelli et al, 2007). The *MOSAICsuite* implements the model-based segmentation methods *Squassh* (Rizk et al, 2014) and *RegionCompetition* (Cardinale et al, 2012) in a plugin for *Fiji* and *ImageJ*, along with model-based spatial pattern and interaction analysis (Shivanandan et al, 2013).

Unsupervised machine-learning approaches are notably implemented in the *BioImageSuite* (Duncan et al, 2004). Supervised machine-learning segmentation is for example implemented in the software *ilastik* (Sommer et al, 2011). *WND-CHARM* (Orlov et al, 2008) uses texture features to classify images without segmenting them. The generic machine-learning library *WEKA* (Hall et al, 2009) is used to provide supervised trainable segmentation in *Fiji*. Again, many application-specific tools exist, like for example the tool *PHANTAST* (Jaccard et al, 2014) for machine-learning-based segmentation of phase-contrast images of adherent cell cultures, which is also available as a plugin for *Fiji* and *ImageJ*.

A frequent use of machine learning is also to post-process results obtained by other image analysis means. This is the approach taken by software tools such as *CellProfiler Analyst* (Jones et al, 2008), *CellClassifier* (Rämö et al, 2009), and *CecogAnalyzer* (Held et al, 2010). More specialized examples include a machine-learning tool to classify different mitochondrial morphologies in wide-field fluorescence microscopy images (Reis et al, 2012), to classify sub-cellular patterns (Huang and Murphy, 2004), and a tool to classify cell cycle states after filter-based segmentation (Wang et al, 2008).

5 Conclusions and discussion

Image analysis in biology is moving from seeing and observing to quantifying and modeling. Interpreting images as scientific measurements, rather than as mere visualizations, brings the need for uncertainty quantification, error analysis, statistical inference frameworks, etc. This raises a number of exciting theoretical and algorithmic questions.

We outlined these questions, focusing on the rapidly developing field of light microscopy, and described three conceptually different paradigms of image analysis, along with popular software tools implementing them. In practice, of course, these approaches are often mixed. It is common, e.g., to use filter-based approaches to compute image features and then use a machine-learning approach on those features in order to detect objects or classify them. Likewise, filters are often included in the forward models of model-based approaches. In fact, filter-based approaches are in some sense also model-based, albeit with an implicit model that is often not evident. Denoising an image using a moving least squares filter (Lancaster and Salkauskas, 1981), for example, is equivalent to maximizing a Gaussian noise likelihood. Another example is the formal link that has been established between the model-based graph-cut framework and the filter-based watershed transform (Couprie et al, 2011). Finally, one can design filters that compute approximate solutions for model-based problems (Gong, 2015). This is not surprising, since ultimately also model-based and machine-learning algorithms are discretized in the computer and hence amount to filters. There is also a blurry boundary between the model-based and machine-learning paradigms. A classical machine-learning approach classifies pixels into "object" vs. "background", based on previously computed features for each pixel. When features use neighborhood information around a pixel, however, there is a conceptual link to Markov random fields (Geman and Geman, 1984) and their model-based Bayesian solution using graph cuts (Delong et al, 2011).

We identified and discussed four main challenges in today's bio-image analysis community: big data, uncertainty quantification, generic algorithms, and collaborative software. To some extent, they mutually entail each other. A big-data project that stores only the final analysis result, for example, critically depends on uncertainty quantification; and both generic algorithms and collaborative software need to be combined to render problem-solving more efficient and prevent reinventing the wheel. The four challenges are hence best addressed jointly.

Addressing these challenges would enable us to work with images like we routinely do with genome and proteome sequences. We could compare images, search image databases by content, and do statistical inference over images. This requires image distance metrics, semantic grammars and annotation, automatic inference systems, query by image content, and probabilistic frameworks over image spaces. All of these are open research areas, and much progress is needed in order to provide robust and generic solutions. The ultimate goal of image analysis is to not operate on the pixel matrix of an image, but on the information represented in the image, independent of the view and the imaging modality chosen. This links syntax and semantics of images on the level of biological meaning, in order to support queries like "find all images of yeast cells in M-phase with gene Cdc11 knocked out". Currently, this only works if the images were manually annotated before (Swedlow and Eliceiri, 2009).

However, even upstream of image annotation open problems remain. One of them is that there are no good forward models for some imaging modalities, including electron microscopy and dark-field microscopy. Another problem is that object models are often *ad hoc* and not true to the biophysics of the sample. While there are occasional works that use physics-based predictive object models (Papademetris et al, 1999; Papademetris, 2000), the computational cost of these models hampers their application. These models are also often black-box with no gradient or structural information available that the optimization algorithm could exploit. This points to the problem that many machine-learning and model-based image-analysis frameworks make implicit assumptions about the features, training data, or models that are used with them. For example, they assume the model to be convex, linear, Gaussian, or separable, which may not be the case for a physics-based simulation. This still requires progress in black-box optimization algorithms (Müller, 2010).

Besides black-box optimization, it could be promising to combine machine-learning and model-based approaches. This would, e.g., make it possible to use machine learning to *learn* the imaging and object models from user-annotated examples, and then use these learned models in a model-based analysis. This would solve the computational cost issue, since machine-learning models are quick to evaluate, and also relax the black-box optimization problem because most machine learning models have an analytical structure with computable gradients. Conversely, model-based approaches could be used to provide ample amounts of simulated training data, to train and validate machine-learning approaches (Murphy, 2012).

A natural way forward is the co-design and co-evolution of mathematical theories of images and inference over images, versatile computer algorithms for image analysis that have few parameters, software implementations thereof that parallelize well and are user friendly, and the biological application defining the level of detail and prior knowledge. These four ingredients need to be balanced and inter-connected. Building on the achievements in the community so far, a quantum leap in computational bio-image analysis and understanding could lie ahead.

6 Acknowledgments

I thank all members of the MOSAIC Group for their creative and scientific contributions and for providing multiple test images and illustration cases for this manuscript. Particular thanks go to Dr. Grégory Paul, Dr. Janick Cardinale, and Dr. Jo Helmuth. This work was supported in parts by the German Federal Ministry of Research and Education (BMBF) under funding code 031A099.

References

Abramoff MD, Magalhães PJ, Ram SJ (2004) Image processing with ImageJ. Biophotonics International 11(7):36–42

Afshar Y, Sbalzarini IF (2016) A parallel distributed-memory particle method enables acquisition-rate segmentation of large fluorescence microscopy images. PLoS One 11(4):e0152,528, DOI 10.1371/journal.pone.0152528

Aigouy B, Farhadifar R, Staple DB, Sagner A, Röper JC, Jülicher F, Eaton S (2010) Cell flow reorients the axis of planar polarity in the wing epithelium of drosophila. Cell 142(5):773–786, DOI 10.1016/j.cell.2010.07.042

Ambühl ME, Brepsant C, Meister JJ, Verkhovsky AB, Sbalzarini IF (2012) High-resolution cell outline segmentation and tracking from phase-contrast microscopy images. J Microsc 245(2):161–170

Andres B, Beier T, Kappes JH (2012) OpenGM: A C++ library for discrete graphical models. arXiv preprint arXiv:12060111

Annibale P, Vanni S, Scarselli M, Rothlisberger U, Radenovic A (2011) Quantitative photo activated localization microscopy: unraveling the effects of photoblinking. PLoS One 6(7):e22,678, DOI 10.1371/journal.pone.0022678

Avidan S (2004) Support vector tracking. IEEE Trans Pattern Anal Machine Intell 26(8):1064–1072

Bar-Shalom Y, Blair WD (eds) (2000) Multitarget/Multisensor Tracking: Applications and Advances, vol III. Artech

Batra D, Yadollahpour P, Guzman-Rivera A, Shakhnarovich G (2012) Diverse M-best solutions in Markov random fields. In: Proc. Europ. Conf. Computer Vision (ECCV), Firenze, Italy, pp 1–16

Bertelli L, Byun J, Manjunath BS (2007) A variational appraoch to exploit prior information in object-background segregation: Application to retinal images. In: Proc. ICIP, IEEE Intl. Conf. Image Processing, vol 6, pp VI–61–VI–64

Berthold MR, Cebron N, Dill F, Gabriel TR, Kötter T, Meinl T, Ohl P, Sieb C, Thiel K, Wiswedel B (2008) KNIME: The Konstanz information miner. Springer

Bishop CM (2007) Pattern Recognition and Machine Learning, 2nd edn. Springer

Blake A, Kohli P, Rother C (2011) Markov Random Fields for Vision and Image Processing. MIT Press

Boykov Y, Veksler O, Zabih R (2001) Fast approximate energy minimization via graph cuts. IEEE Trans Pattern Anal Machine Intell 23:1222–1239, DOI http://doi.ieeecomputersociety.org/10.1109/34.969114

Bradski G, Kaehler A (2008) Learning OpenCV: Computer vision with the OpenCV library. O'Reilly

Breiman L (2001) Random forests. Machine Learning 45:5–32

Brown ES, Chan TF, Bresson X (2011) Completely convex formulation of the Chan-Vese image segmentation model. Int J Comput Vis DOI 10.1007/s11263-011-0499-y

Canny J (1986) A computational approach to edge detection. IEEE Trans Pattern Anal Machine Intell 8(6):679–698

Cardinale J (2013) Unsupervised segmentation and shape posterior estimation under Bayesian image models. PhD thesis, Diss. ETH No. 21026, MOSAIC Group, ETH Zürich

Cardinale J, Rauch A, Barral Y, Székely G, Sbalzarini IF (2009) Bayesian image analysis with on-line confidence estimates and its application to microtubule tracking. In: Proc. IEEE Intl. Symposium Biomedical Imaging (ISBI), IEEE, Boston, USA, pp 1091–1094

Cardinale J, Paul G, Sbalzarini IF (2012) Discrete region competition for unknown numbers of connected regions. IEEE Trans Image Process 21(8):3531–3545

Cardona A, Tomancak P (2012) Current challenges in open-source bioimage informatics. Nat Methods 9(7):661–665

Carpenter AE, Jones TR, Lamprecht MR, Clarke C, Kang IH, Friman O, Guertin DA, Chang JH, Lindquist RA, Moffat J, et al (2006) Cellprofiler: image analysis software for identifying and quantifying cell phenotypes. Genome biology 7(10):R100

Carpenter AE, Kamentsky L, Eliceiri KW (2012) A call for bioimaging software usability. Nat Methods 9(7):666–670

Chan TF, Shen JJ (2005) Image Processing and Analysis: Variational, PDE, Wavelet, and Stochastic Methods. SIAM

Chang J, Fisher III JW (2011) Efficient MCMC sampling with implicit shape representations. In: Computer Vision and Pattern Recognition (CVPR), IEEE Conference on, IEEE, IEEE, pp 2081–2088

de Chaumont F, Dallongeville S, Olivo-Marin JC (2011) ICY: a new open-source community image processing software. In: Proc. IEEE Intl. Symposium Biomedical Imaging (ISBI), pp 234–237

de Chaumont F, Dallongeville S, Chenouard N, Hervé N, Pop S, Provoost T, Meas-Yedid V, Pankajakshan P, Lecomte T, Le Montagner Y, Lagache T, Dufour A, Olivo-Marin JC (2012) Icy: an open bioimage informatics platform for extended reproducible research. Nat Methods 9(7):690–696, DOI 10.1038/nmeth.2075

Chenouard N, Smal I, de Chaumont F, Maška M, Sbalzarini IF, Gong Y, Cardinale J, Carthel C, Coraluppi S, Winter M, Cohen AR, Godinez WJ, Rohr K, Kalaidzidis Y, Liang L, Duncan J, Shen H, Xu Y, Magnusson KEG, Jaldén J, Blau HM, Paul-Gilloteaux P, Roudot P, Kervrann C, Waharte F, Tinevez JY, Shorte SL, Willemse J, Celler K, van Wezel GP, Dan HW, Tsai YS, de Solórzano CO, Olivo-Marin JC, Meijering E (2014) Objective comparison of particle tracking methods. Nat Methods 11(3):281–289, DOI 10.1038/nmeth.2808

Cherkassky VS, Mulier F (1998) Learning from data. J. Wiley & Sons

Chesnaud C, Réfrégier P, Boulet W (1999) Statistical region snake-based segmentation adapted to different physical noise models. IEEE Trans Pattern Anal Machine Intell 21(11):1145–1157

Ciresan D, Meier U, Schmidhuber J (2012) Multi-column deep neural networks for image classification. In: Proc. IEEE Intl. Conf. Computer Vision and Pattern Recognition (CVPR), IEEE, pp 3642–3649

Clack NG, O'Connor DH, Huber D, Petreanu L, Hires A, Peron S, Svoboda K, Myers EW (2012) Automated tracking of whiskers in videos of head fixed rodents. PLoS Comput Biol 8(7):e1002,591, DOI 10.1371/journal.pcbi.1002591

Collinet C, Stöter M, Bradshaw CR, Samusik N, Rink JC, Kenski D, Habermann B, Buchholz F, Henschel R, Mueller MS, Nagel WE, Fava E, Kalaidzidis Y, Zerial M (2010) Systems survey of endocytosis by multiparametric image analysis. Nature 464:243–249

Cooley JW, Tukey JW (1965) An algorithm for the machine calculation of complex Fourier series. Math Comput 19(90):297–301

Couprie C, Grady L, Najman L, Talbot H (2011) Power watershed: A unifying graph-based optimization framework. IEEE Trans Pattern Anal Machine Intell 33(7):1384–1399

Cox IJ, Hingorani SL (1996) An efficient implementation of Reid's multiple hypothesis tracking algorithm and its evaluation for the purpose of visual tracking. IEEE Trans Pattern Anal 18(2):138–150

Crocker JC, Grier DG (1996) Methods of digital video microspopy for colloidal studies. J Colloid Interf Sci 179:298–310

Crosier M, Griffin LD (2010) Using basic image features for texture classification. International Journal of Computer Vision 88(3):447–460

Danuser G (2011) Computer vision in cell biology. Cell 147(5):973–978, DOI 10.1016/j.cell.2011.11.001

Delong A, Osokin A, Isack HN, Boykov Y (2011) Fast approximate energy minimization with label costs. Int J Comput Vis 96(1):1–27

Demirel O, Smal I, Niessen WJ, Meijering E, Sbalzarini IF (2014a) An adaptive distributed resampling algorithm with non-proportional allocation. In: Proc. ICASSP, IEEE Intl. Conf. Acoustics, Speech, and Signal Processing, IEEE, IEEE, Florence, Italy, pp 1635–1639

Demirel O, Smal I, Niessen WJ, Meijering E, Sbalzarini IF (2014b) Piecewise constant sequential importance sampling for fast particle filtering. In: Proc. 10th IET Conf. Data Fusion & Target Tracking, IET, Liverpool, UK

Demirel O, Smal I, Niessen WJ, Meijering E, Sbalzarini IF (2014c) PPF – A parallel particle filtering library. In: Proc. 10th IET Conf. Data Fusion & Target Tracking, IET, Liverpool, UK

Dietrich CF (1991) Uncertainty, Calibration and Probability: The Statistics of Scientific and Industrial Measurement, 2nd edn. Measurement Science and Technology, Adam Hilger

Duda RO, Hart PE, Stork DG (2000) Pattern Classification, 2nd edn. John Wiley & Sons, New York

Duncan JS, Papademetris X, Yang J, Jackowski M, Zeng X, Staib LH (2004) Geometric strategies for neuroanatomic analysis from MRI. Neuroimage 23 Suppl. 1:S34–S45, DOI 10.1016/j.neuroimage.2004.07.027

Dzyubachyk O, van Cappellen WA, Essers J, Niessen WJ, Meijering E (2010) Advanced level-set-based cell tracking in time-lapse fluorescence microscopy. IEEE Trans Med Imaging 29(3):852–867

Eils R, Athale C (2003) Computational imaging in cell biology. J Cell Biol 161(3):477–481

El-Naqa I, Yang Y, Wernick MN, Galatsanos NP, Nishikawa RM (2002) A support vector machine approach for detection of microcalcifications. IEEE Trans Med Imaging 21(12):1552–1563

El-Zehiry N, Elmaghraby A (2009) An active surface model for volumetric image segmentation. In: Proc. IEEE Intl. Symposium Biomedical Imaging (ISBI), pp 1358–1361

Eliceiri KW, Berthold MR, Goldberg IG, Ibáñez L, Manjunath BS, Martone ME, Murphy RF, Peng H, Plant AL, Roysam B, Stuurmann N, Swedlow JR, Tomancak P, Carpenter AE (2012) Biological imaging software tools. Nat Methods 9(7):697–710, DOI 10.1038/nmeth.2084

Engelbrecht C, Stelzer E (2006) Resolution enhancement in a light-sheet-based microscope (SPIM). Opt Lett 31:1477–1479

Etyngier P, Ségonne F, Keriven R (2007) Shape priors using manifold learning techniques. In: Proc. IEEE Intl. Conf. Computer Vision (ICCV), IEEE, pp 1–8

Ewers H, Smith AE, Sbalzarini IF, Lilie H, Koumoutsakos P, Helenius A (2005) Single-particle tracking of murine polyoma virus-like particles on live cells and artificial membranes. Proc Natl Acad Sci USA 102(42):15,110–15,115

Farhadifar R, Röper JC, Aigouy B, Eaton S, Jülicher F (2007) The influence of cell mechanics, cell-cell interactions, and proliferation on epithelial packing. Curr Biol 17(24):2095–2104, DOI 10.1016/j.cub.2007.11.049

Fuchs TJ, Wild PJ, Moch H, Buhmann JM (2008) Computational pathology analysis of tissue microarrays predicts survival of renal clear cell carcinoma patients. In: Lect. Notes Comput. Sc., vol 5242, pp 1–8

Fuchs TJ, Haybaeck J, Wild PJ, Heikenwalder M, Moch H, Aguzzi A, Buhmann JM (2009) Randomized tree ensembles for object detection in computational pathology. In: Proc. Intl. Symp. Visual Comput. (ISVC), pp 367–378

Galizia A, D'Agostino D, Clematis A (2015) An MPI–CUDA library for image processing on HPC architectures. J Comput Appl Mech 273:414–427

Geman S, Geman D (1984) Stochastic relaxation, Gibbs distributions, and the Bayesian restoration of images. IEEE Trans Pattern Anal Machine Intell 6(6):721–741

Genovesio A, Olivo-Marin JC (2004) Split and merge data association filter for dense multi-target tracking. In: Proceedings of the 17th International Conference on Pattern Recognition (ICPR'04), IEEE, vol 4, pp 677–680

Gong Y (2015) Spectrally regularized surfaces. PhD thesis, Diss. ETH No. 22616, MOSAIC Group, ETH Zürich

Gong Y, Sbalzarini IF (2014) Image enhancement by gradient distribution specification. In: Jawahar CV, Shan S (eds) Computer Vision – ACCV 2014 Workshops, Revised Selected Papers, Part II, Springer, Singapore, Lect. Notes Comput. Sci., vol 9009, pp 47–62

Hall M, Frank E, Holmes G, Pfahringer B, Reutemann P, Witten IH (2009) The WEKA data mining software: an update. SIGKDD Explor Newsl 11(1):10–18, DOI 10.1145/1656274.1656278, URL http://doi.acm.org/10.1145/1656274.1656278

Halpern JY (2005) Reasoning about Uncertainty. MIT Press

Hecht E (2001) Optics, 4th edn. Addison Wesley

Held M, Schmitz MHA, Fischer B, Walter T, Neumann B, Olma MH, Peter M, Ellenberg J, Gerlich DW (2010) CellCognition: time-resolved phenotype annotation in high-throughput live cell imaging. Nature methods 7(9):747–754

Helmuth JA, Sbalzarini IF (2009) Deconvolving active contours for fluorescence microscopy images. In: Proc. Intl. Symp. Visual Computing (ISVC), Springer, Las Vegas, USA, Lecture Notes in Computer Science, vol 5875, pp 544–553

Helmuth JA, Burckhardt CJ, Koumoutsakos P, Greber UF, Sbalzarini IF (2007) A novel supervised trajectory segmentation algorithm identifies distinct types of human adenovirus motion in host cells. J Struct Biol 159(3):347–358

Helmuth JA, Burckhardt CJ, Greber UF, Sbalzarini IF (2009) Shape reconstruction of subcellular structures from live cell fluorescence microscopy images. J Struct Biol 167:1–10

Helmuth JA, Paul G, Sbalzarini IF (2010) Beyond co-localization: inferring spatial interactions between sub-cellular structures from microscopy images. BMC Bioinformatics 11:372

Hong Y, Kwong S, Chang Y, Ren Q (2008) Consensus unsupervised feature ranking from multiple views. Pattern Recognition Lett 29:595–602

Huang K, Murphy RF (2004) Automated classification of subcellular patterns in multicell images without segmentation into single cells. In: Proc. IEEE Intl. Symposium Biomedical Imaging (ISBI), pp 1139–1142

Hue C, Le Cadre JP, Pérez P (2002) Tracking multiple objects with particle filtering. IEEE Trans Aerospace Electronic Systems 38(3):791–812

Huisken J, Swoger J, Del Bene F, Wittbrodt J, Stelzer EHK (2004) Optical sectioning deep inside live embryos by selective plane illumination microscopy. Science 305:1007–1009

Ibanez L, Schroeder W, Ng L, Cates J (2005) The ITK Software Guide. Kitware, Inc. ISBN 1-930934-15-7, http://www.itk.org/ItkSoftwareGuide.pdf, 2nd edn

Jaccard N, Griffin LD, Keser A, Macown RJ, Super A, Veraitch FS, Szita N (2014) Automated method for the rapid and precise estimation of adherent cell culture characteristics from phase contrast microscopy images. Biotechnology and bioengineering 111(3):504–517

Jancsary J, Nowozin S, Sharp T, Rother C (2012) Regression tree fields–an efficient, non-parametric approach to image labeling problems. In: Proc. Computer Vision and Pattern Recognition (CVPR), 2012 IEEE Conference on, IEEE, pp 2376–2383

Jaqaman K, Loerke D, Mettlen M, Kuwata H, Grinstein S, Schmid S, Danuser G (2008) Robust single-particle tracking in live-cell time-lapse sequences. Nat Methods 5:695–702, DOI DOI 10.1038/nmeth.1237

Jones TR, Kang IH, Wheeler DB, Lindquist RA, Papallo A, Sabatini DM, Golland P, Carpenter AE (2008) CellProfiler Analyst: data exploration and analysis software for complex image-based screens. BMC Bioinformatics 9:482, DOI 10.1186/1471-2105-9-482

Jung M, Chung G, Sundaramoorthi G, Vese L, Yuille A (2009) Sobolev gradients and joint variational image segmentation, denoising and deblurring. In: SPIE Electronic Imaging Conference Proceedings, Computational Imaging VII, SPIE, vol 7246

Kalaidzidis Y (2007) Intracellular objects tracking. Eur J Cell Biol 86(9):569–578, DOI 10.1016/j.ejcb.2007.05.005

Kalaidzidis Y (2009) Multiple objects tracking in fluorescence microscopy. J Math Biol 58(1-2):57–80, DOI 10.1007/s00285-008-0180-4

Kankaanpää P, Paavolainen L, Tiitta S, Karjalainen M, Päivärinne J, Nieminen J, Marjomäki V, Heino J, White DJ (2012) BioImageXD: an open, general-purpose and high-throughput image-processing platform. Nat Methods 9(7):683—689, DOI 10.1038/nmeth.2047

Kannala J, Rahtu E (2012) BSIF: Binarized statistical image features. In: Proc. 21st Intl. Conf. Pattern Recognition (ICPR), IEEE, pp 1363–1366

Kass M, Witkin A, Terzopoulos D (1988) Snakes: Active contour models. Int J Comput Vis pp 321–331

Kaynig V, Fuchs T, Buhmann JM (2010) Neuron geometry extraction by perceptual grouping in ssTEM images. In: Proc. IEEE Intl. Conf. Computer Vision and Pattern Recognition (CVPR), pp 2902–2909

Kohli P, Lempitsky V, Rother C (2010) Uncertainty driven multi-scale optimization. In: Proc. DAGM, Pattern Recognition, Springer, Darmstadt, Germany

Köthe U (1999) Reusable software in computer vision. In: Jähne B, Haußecker H, Geißler P (eds) Handbook on Computer Vision and Applications, vol 3, Academic Press, chap 6, pp 105–134

Kvilekval K, Fedorov D, Obara B, Singh A, Manjunath BS (2010) Bisque: a platform for bioimage analysis and management. Bioinformatics 26(4):544–552, DOI 10.1093/bioinformatics/btp699

Lagache T, Lang G, Sauvonnet N, Olivo-Marin JC (2013) Analysis of the spatial organization of molecules with robust statistics. PLoS One 8(12):e80,914, DOI 10.1371/journal.pone.0080914

Lagache T, Sauvonnet N, Danglot L, Olivo-Marin JC (2015) Statistical analysis of molecule colocalization in bioimaging. Cytometry A

Lamprecht M, Sabatini DM, Carpenter AE (2007) CellProfiler: free, versatile software for automated biological image analysis. BioTechniques 42(1):71–75

Lancaster P, Salkauskas K (1981) Surfaces generated by moving least squares methods. Math Comput 37(155):141–158

Le Maître OP, Knio OM (2010) Spectral Methods for Uncertainty Quantification. Springer

Li K, Miller ED, Weiss LE, Campbell PG, Kanade T (2006) Online tracking of migrating and proliferating cells imaged with phase-contrast microscopy. In: IEEE Proceedings of the 2006 Conference on Computer Vision and Pattern Recognition Workshop (CVPRW), IEEE Computer Society, pp 65–72

Li K, Chen M, Kanade T (2007) Cell population tracking and lineage construction with spatiotemporal context. Med Image Comput Comput Assist Interv Int Conf Med Image Comput Comput Assist Interv 10(Pt 2):295–302

Li S, Kwok JT, Zhu H, Wang Y (2003) Texture classification using the support vector machines. Pattern Recognition 36:2883–2893

Lin G, Adiga U, Olson K, Guzowski JF, Barnes CA, Roysam B (2003) A hybrid 3d watershed algorithm incorporating gradient cues and object models for automatic segmentation of nuclei in confocal image stacks. Cytometry A 56(1):23–36

Linfoot EH, Wolf E (1956) Phase distribution near focus in an aberration-free diffraction image. Proc, Phys Soc B 69(8):823–832

Lowe DG (1999) Object recognition from local scale-invariant features. In: Proc. 7th Intl. Conf. Computer Vision (ICCV), IEEE, vol 2, pp 1150–1157

Machacek M, Danuser G (2006) Morphodynamic profiling of protrusion phenotypes. Biophys J 90:1439–1452

Manders EMM, Hoebe R, Strackee J, Vossepoel AM, Aten JA (1996) Largest contour segmentation: a tool for the localization of spots in confocal images. Cytometry 23(1):15–21

Marjoram P, Molitor J, Plagnol V, Tavare S (2003) Markov chain Monte Carlo without likelihoods. Proc Natl Acad Sci USA 100(26):15,324–15,328

Martin P, Gier PR, Goudail F, Guérault F (2004) Influence of the noise model on level set active contour segmentation. IEEE Trans Pattern Anal Machine Intell 26(6):799–803

Maška M, Ulman V, Svoboda D, Matula P, Matula P, Ederra C, Urbiola A, España T, Venkatesan S, Balak DMW, Karas P, Bolcková T, Štreitová M, Carthel C, Coraluppi S, Harder N, Rohr K, Magnusson KEG, Jaldén J, Blau HM, Dzyubachyk O, Křížek P, Hagen GM, Pastor-Escuredo D, Jimenez-Carretero D, Ledesma-Carbayo MJ, Muñoz Barrutia A, Meijering E, Kozubek M, Ortiz-de Solorzano C (2014) A benchmark for comparison of cell tracking algorithms. Bioinformatics 30(11):1609–1617

McCann MT, Bhagavatula R, Fickus MC, Ozolek JA, Kovacevic J (2012) Automated colitis detection from endoscopic biopsies as a tissue screening tool in diagnostic pathology. In: Proc. Image Processing (ICIP), 2012 19th IEEE International Conference on, IEEE, pp 2809–2812

Meyer F, Vachier C, Oliveras A, Salembier P (1997) Morphological tools for segmentation: Connected filters and watersheds. Annales des télécommunications 52(7-8):367–379

Müller CL (2010) Black-box landscapes: Characterization, optimization, sampling, and application to geometric configuration problems. PhD thesis, Diss. ETH No. 19438, ETH Zürich

Murphy RF (2012) CellOrganizer: Image-derived models of subcellular organization and protein distribution. Methods Cell Biol 110:179–193, DOI 10.1016/B978-0-12-388403-9.00007-2

Myers G (2012) Why bioimage informatics matters. Nat Methods 9(7):659–660

Najman L, Schmitt M (1996) Geodesic saliency of watershed contours and hierarchical segmentation. IEEE Trans Pattern Anal Machine Intell 18(12):1163–1173

Najman L, Talbot H (2010) Mathematical Morphology. John Wiley & Sons

Nandy K (2015) Segmentation and informatics in multidimensional fluorescence optical microscopy images. Ph.D. thesis, University of Maryland

Nicolescu C, Jonker P (2000) Parallel low-level image processing on a distributed-memory system. In: Rolim J (ed) Parallel and Distributed Processing, Lecture Notes in Computer Science, vol 1800, Springer, pp 226–233, DOI 10.1007/3-540-45591-4_30, URL http://dx.doi.org/10.1007/3-540-45591-4_30

Nilufar S, Perkins TJ (2014) Learning to detect contours with dynamic programming snakes. In: Proc. IEEE Intl. Conf. Pattern Recognition (ICPR), IEEE, pp 984–989

North AJ (2006) Seeing is believing? a beginners' guide to practical pitfalls in image acquisition. J Cell Biol 172(1):9–18, DOI 10.1083/jcb.200507103

Ober RJ, Tahmasbi A, Ram S, Lin Z, Ward ES (2015) Quantitative aspects of single-molecule microscopy – information-theoretic analysis of single-molecule data. IEEE Signal Proc Mag 32(1):58–69

Olivo-Marin JC (2002) Extraction of spots in biological images using multiscale products. Pattern recognition 35(9):1989–1996

Orlov N, Shamir L, Macura T, Johnston J, Eckley DM, Goldberg IG (2008) WND-CHARM: Multi-purpose image classification using compound image transforms. Pattern Recognition Letters 29(11):1684 – 1693, DOI 10.1016/j.patrec.2008.04.013, URL http://www.sciencedirect.com/science/article/pii/S0167865508001530

Orlov NV, Chen WW, Eckley DM, Macura TJ, Shamir L, Jaffe ES, Goldberg IG (2010) Automatic classification of lymphoma images with transform-based global features. IEEE Trans Information Technol in Biomedicine 14(4):1003–1013

Otsu N (1975) A threshold selection method from gray-level histograms. Automatica 11(285-296):23–27

Ovaska K, Laakso M, Haapa-Paananen S, Louhimo R, Chen P, Aittomäki V, Valo E, Núñez-Fontarnau J, Rantanen V, Karinen S, Nousiainen K, Lahesmaa-Korpinen AM, Miettinen M, Saarinen L, Kohonen P, Wu J, Westermarck J, Hautaniemi S (2010) Large-scale data integration framework provides a comprehensive view on glioblastoma multiforme. Genome Med 2(9):65

Papademetris X (2000) Estimation of 3D left ventricular deformation from medical images using biomechanical models. Ph.D.. thesis, Yale University

Papademetris X, Sinusas AJ, Dione DP, Duncan JS (1999) 3d cardiac deformation from ultrasound images. In: Proc. MICCAI, Medical Image Computing and Computer-Assisted Intervention, pp 420–429

Paul G, Cardinale J, Sbalzarini IF (2011) An alternating split Bregman algorithm for multi-region segmentation. In: Proc. 45th IEEE Asilomar Conf. Signals, Systems, and Computers, IEEE, Asilomar, CA, USA, pp 426–430

Paul G, Cardinale J, Sbalzarini IF (2013) Coupling image restoration and segmentation: A generalized linear model/Bregman perspective. Int J Comput Vis 104(1):69–93, URL 10.1007/s11263-013-0615-2

Peng H (2008) Bioimage informatics: a new area of engineering biology. Bioinformatics 24(17):1827–1836, DOI 10.1093/bioinformatics/btn346

Peng H, Ruan Z, Long F, Simpson JH, Myers EW (2010) V3D enables real-time 3D visualization and quantitative analysis of large-scale biological image data sets. Nat Biotechnol 28(4):348–353, DOI 10.1038/nbt.1612

Peng H, Bria A, Zhou Z, Iannello G, Long F (2014) Extensible visualization and analysis for multidimensional images using Vaa3D. Nature protocols 9(1):193–208

Perona P, Malik J (1990) Scale-space and edge detection using anisotropic diffusion. IEEE Trans Pattern Anal Machine Intell 12(7):629–639

Pock T, Cremers D, Bischof H, Chambolle A (2009) An algorithm for minimizing the Mumford-Shah functional. In: Proc. IEEE Intl. Conf. Computer Vision (ICCV), pp 1133–1140, DOI 10.1109/ICCV.2009.5459348

Rajaram S, Pavie B, Hac NEF, Altschuler SJ, Wu LF (2012) SimuCell: a flexible framework for creating synthetic microscopy images. Nat Methods 9(7):634–635

Ramakrishna V, Batra D (2012) Mode-marginals: Expressing uncertainty via diverse M-best solutions. In: Proc. NIPS, Neural Information Processing Systems Foundation, Lake Tahoe, Nevada, USA

Rämö P, Sacher R, Snijder B, Begemann B, Pelkmans L (2009) CellClassifier: supervised learning of cellular phenotypes. Bioinformatics 25(22):3028–3030, DOI 10.1093/bioinformatics/btp524

Rantanen V, Valori M, Hautaniemi S (2014) Anima: modular workflow system for comprehensive image data analysis. Front Bioeng Biotechnol 2:25

Reddick WE, Glass JO, Cook EN, Elkin TD, Deaton RJ (1997) Automated segmentation and classification of multispectral magnetic resonance images of brain using artificial neural networks. IEEE Trans Med Imaging 16(6):911–918

Reis Y, Bernardo-Faura M, Richter D, Wolf T, Brors B, Hamacher-Brady A, Eils R, Brady NR (2012) Multi-parametric analysis and modeling of relationships between mitochondrial morphology and apoptosis. PLoS One 7(1):e28,694, DOI 10.1371/journal.pone.0028694

Barbier de Reuille P, Routier-Kierzkowska AL, Kierzkowski D, Bassel GW, Schüpbach T, Tauriello G, Bajpai N, Strauss S, Weber A, Kiss A, Burian A, Hofhuis H, Sapala A, Lipowczan M, Heimlicher MB, Robinson S, Bayer EM, Basler K, Koumoutsakos P, Roeder AHK, Aegerter-Wilmsen T, Nakayama N, Tsiantis M, Hay A, Kwiatkowska D, Xenarios I, Kuhlemeier C, Smith RS (2015) MorphoGraphX: A platform for quantifying morphogenesis in 4D. Elife 4:e05,864, DOI 10.7554/eLife.05864

Rex DE, Ma JQ, Toga AW (2003) The LONI pipeline processing environment. Neuroimage 19(3):1033–1048

Reynaud EG, Peychl J, Huisken J, Tomancak P (2014) Guide to light-sheet microscopy for adventurous biologists. Nat Methods 12(1):30–34

Rizk A, Paul G, Incardona P, Bugarski M, Mansouri M, Niemann A, Ziegler U, Berger P, Sbalzarini IF (2014) Segmentation and quantification of subcellular structures in fluorescence microscopy images using Squassh. Nature Protocols 9(3):586–596

Royer LA, Weigert M, Günther U, Maghelli N, Jug F, Sbalzarini IF, Myers EW (2015) ClearVolume: open-source live 3D visualization for light-sheet microscopy. Nat Methods 12(6):480–481

Roysam B, Shain W, Robey E, Chen Y, Narayanaswamy A, Tsai CL, Al-Kofahi Y, Bjornsson C, Ladi E, Herzmark P (2008) The FARSIGHT project: Associative 4D/5D image analysis methods for quantifying complex and dynamic biological microenvironments. Microscopy and Microanalysis 14(S2):60–61

Ruhnow F, Zwicker D, Diez S (2011) Tracking single particles and elongated filaments with nanometer precision. Biophys J 100(11):2820–2828

Ruprecht V, Axmann M, Wieser S, Schütz GJ (2011) What can we learn from single moecule trajectories? Curr Protein & Peptide Sci 12(8):714–724

Sbalzarini IF (2010) Abstractions and middleware for petascale computing and beyond. Intl J Distr Systems & Technol 1(2):40–56

Sbalzarini IF (2013) Modeling and simulation of biological systems from image data. Bioessays 35(5):482–490, DOI 10.1002/bies.201200051

Sbalzarini IF, Koumoutsakos P (2005) Feature point tracking and trajectory analysis for video imaging in cell biology. J Struct Biol 151(2):182–195

Schiegg M, Hanslovsky P, Kausler BX, Hufnagel L, Hamprecht F (2013) Conservation tracking. In: Proc. IEEE Intl. Conf. Computer Vision (ICCV), IEEE, pp 2928–2935

Schindelin J (2008) Fiji is just ImageJ (batteries included). In: ImageJ User and Developer Conference

Schindelin J, Arganda-Carreras I, Frise E, Kaynig V, Longair M, Pietzsch T, Preibisch S, Rueden C, Saalfeld S, Schmid B, Tinevez JY, White DJ, Hartenstein V, Eliceiri K, Tomancak P, Cardona A (2012) Fiji: an open-source platform for biological-image analysis. Nat Methods 9(7):676–682, DOI 10.1038/nmeth.2019

Schneider CA, Rasband WS, Eliceiri KW (2012) NIH Image to ImageJ: 25 years of image analysis. Nat Methods 9(7):671–675

Schölkopf B, Smola AJ (2002) Learning with Kernels. Support Vector Machines, Regularization, Optimization, and Beyond. MIT Press, Cambridge, Massachusetts

Seinstra FJ, Koelma D, Geusebroek JM (2002) A software architecture for user transparent parallel image processing. Parallel Computing 28(7–8):967–993, DOI http://dx.doi.org/10.1016/S0167-8191(02)00103-5, URL http://www.sciencedirect.com/science/article/pii/S0167819102001035

Sethian JA (1999) Level Set Methods and Fast Marching Methods. Cambridge University Press, Cambridge, UK

Shafer G (1976) A Mathematical Theory of Evidence. Princeton University Press

Shamir L, Delaney JD, Orlov N, Eckley DM, Goldberg IG (2010) Pattern recognition software and techniques for biological image analysis. PLoS Comput Biol 6(11):e1000,974, DOI 10.1371/journal.pcbi.1000974

Shi Y, Karl W (2005) Real-time tracking using level sets. In: Proc. IEEE Conf. CVPR, vol 2, pp 34–41, DOI 10.1109/CVPR.2005.294

Shivanandan A, Radenovic A, Sbalzarini IF (2013) MosaicIA: an ImageJ/Fiji plugin for spatial pattern and interaction analysis. BMC Bioinformatics 14:349

Smal I, Meijering E, Draegestein K, Galjart N, Grigoriev I, Akhmanova A, van Royen ME, Houtsmuller AB, Niessen W (2008) Multiple object tracking in molecular bioimaging by Rao-Blackwellized marginal particle filtering. Med Image Anal 12(6):764–777, DOI 10.1016/j.media.2008.03.004

Snijder B, Sacher R, Rämö P, Damm EM, Liberali P, Pelkmans L (2009) Population context determines cell-to-cell variability in endocytosis and virus infection. Nature 461(7263):520–523, DOI 10.1038/nature08282

Sommer C, Strähle C, Köthe U, Hamprecht FA (2011) ilastik: interactive learning and segmentation toolkit. In: Proc. IEEE Intl. Symposium Biomedical Imaging (ISBI), pp 230–233

Stoeckli M, Chaurand P, Hallahan DE, Caprioli RM (2001) Imaging mass spectrometry: A new technology for the analysis of protein expression in mammalian tissues. Nat Medicine 7(4):493–496

Swedlow JR, Eliceiri KW (2009) Open source bioimage informatics for cell biology. Trends Cell Biol 19(11):656–660, DOI 10.1016/j.tcb.2009.08.007

Swedlow JR, Goldberg I, Brauner E, Sorger PK (2003) Informatics and quantitative analysis in biological imaging. Science 300:100–102

Tomer R, Khairy K, Amat F, Keller PJ (2012) Quantitative high-speed imaging of entire developing embryos with simultaneous multiview light-sheet microscopy. Nat Methods 9(7):755–763, DOI 10.1038/nmeth.2062

Vallotton P, Ponti A, Waterman-Storer CM, Salmon ED, Danuser G (2003) Recovery, visualization, and analysis of actin and tubulin polymer flow in live cells: A fluorescent speckle microscopy study. Biophys J 85:1289–1306

Vebjorn L, Sokolnicki KL, Carpenter AE (2012) Annotated high-throughput microscopy image sets for validation. Nat Methods 9(7):637

Wang M, Zhou X, Li F, Huckins J, King RW, Wong STC (2008) Novel cell segmentation and online SVM for cell cycle phase identification in automated microscopy. Bioinformatics 24(1):94–101, DOI 10.1093/bioinformatics/btm530

Weber M, Huisken J (2012) Omnidirectional microscopy. Nat Methods 9(7):656–657

Wieser S, Schütz GJ (2008) Tracking single molecules in the live cell plasma membrane–do's and don't's. Methods 46(2):131–140, DOI 10.1016/j.ymeth.2008.06.010

Wieser S, Axmann M, Schütz GJ (2008) Versatile analysis of single-molecule tracking data by comprehensive testing against monte carlo simulations. Biophys J 95(12):5988–6001, DOI 10.1529/biophysj.108.141655

Willert CE, Gharib M (1991) Digital particle image velocimetry. Experiments in Fluids 10:181–193

Williams O, Blake A, Cipolla R (2005) Sparse Bayesian learning for efficient visual tracking. IEEE Trans Pattern Anal Machine Intell 27(8):1292–1304

Witkin A (1984) Scale-space filtering: A new approach to multi-scale description. In: Proc. Acoustics, Speech, and Signal Processing (ICASSP), IEEE International Conference on, IEEE, vol 9, pp 150–153, URL 10.1109/ICASSP.1984.1172729

Witteveen JAS, Iaccarino G (2012) Simplex stochastic collocation with random sampling and extrapolation for nonhypercube probability spaces. SIAM J Sci Comput 34(2):A814–A838

Xiao X, Geyer VF, Bowne-Anderson H, Howard J, Sbalzarini IF (2016) Automatic optimal filament segmentation with sub-pixel accuracy using generalized linear models and B-spline level-sets. Med Image Anal 32:157–172

Xiu D (2009) Fast numerical methods for stochastic computations: A review. Commun Comput Phys 5:242–272

Xiu D, Karniadakis GEM (2002) The Wiener-Askey polynomial chaos for stochastic differential equations. SIAM J Sci Comput 24(2):619–644

Xu C, Corso JJ (2012) Evaluation of super-voxel methods for early video processing. In: Proc. Computer Vision and Pattern Recognition (CVPR), 2012 IEEE Conference on, IEEE, Providence, pp 1202–1209, URL 10.1109/CVPR.2012.6247802

Yamauchi Y, Boukari H, Banerjee I, Sbalzarini IF, Horvath P, Helenius A (2011) Histone deacetylase 8 is required for centrosome cohesion and influenza A virus entry. PLoS Pathog 7(10):e1002,316

Yin Z, Li K, Kanade T, Chen M (2010) Understanding the optics to aid microscopy image segmentation. In: Proc. MICCAI, Medical Image Computing and Computer-Assisted Intervention, Springer, pp 209–217

Yushkevich PA, Piven J, Cody Hazlett H, Gimpel Smith R, Ho S, Gee JC, Gerig G (2006) User-guided 3D active contour segmentation of anatomical structures: Significantly improved efficiency and reliability. NeuroImage 31(3):1116–1128

Zhang B, Zerubia J, Olivo-Marin JC (2007) Gaussian approximations of fluorescence microscope point-spread function models. Appl Opt 46(10):1819–1829

Zhou J, Chan KL, Chong VFH, Krishnan SM (2005) Extraction of brain tumor from MR images using one-class support vector machine. In: Proc. IEEE Engineering in Medicine and Biology, Annual Conference, Shanghai, China, pp 6411–6414

Zhu SC, Yuille A (1996) Region competition: Unifying snakes, region growing, and Bayes/MDL for multiband image segmentation. IEEE Trans Pattern Anal Machine Intell 18(9):884–900